Transient receptor potential canonical type 3 channels facilitate endothelium-derived hyperpolarization-mediated resistance artery vasodilator activity

Sevvandi Senadheera[1,*] Youngsoo Kim[1], T Hilton Grayson[1], Sianne Toemoe[1], Mikhail Y Kochukov[2], Joel Abramowitz[3], Gary D Housley[1], Rebecca L Bertrand[1], Preet S Chadha[1,4], Paul P Bertrand[1], Timothy V Murphy[1], Marianne Tare[6], Lutz Birnbaumer[3], Sean P Marrelli[2,5,#] and Shaun L Sandow[1,*#]

[1]Department of Physiology, School of Medical Sciences, Faculty of Medicine, University of New South Wales, Sydney, 2052, Australia

[2]Department of Anesthesiology, Baylor College of Medicine, Houston, TX, USA

[3]Transmembrane Signalling Group, Laboratory of Neurobiology, National Institute of Environmental Health Sciences, NIH, Research Triangle Park, North Carolina, USA

[4]Pharmacology and Cell Physiology, Division of Biomedical Sciences, St George's, University of London, Cranmer Terrace, London, SW17 0RE, UK

[5]Department of Physiology and Biophysics and Graduate Program in Physiology, Cardiovascular Sciences Track, Baylor College of Medicine, Houston, TX, USA

[6]Department of Physiology, Monash University, Melbourne, 3800, Australia

*Corresponding authors

Sevvandi Senadheera, Pharmacology and Physiology, School of Medical Sciences, Faculty of Medicine, University of New South Wales, NSW, Sydney, 2052, Australia

Fax. + 61 2 9385 1059. Ph. + 61 2 9385 8490. email: s.senadheera@student.unsw.edu.au

and

Shaun L. Sandow, Pharmacology, School of Medical Sciences, Faculty of Medicine, University of New South Wales, NSW, Sydney, 2052, Australia

Fax. + 61 2 9385 1059. Ph. + 61 2 9385 2556. email: shaun.sandow@unsw.edu.au

[#]Equal contributors

Abstract

Aims. Microdomain signalling mechanisms underlie key aspects of artery function and the modulation of intracellular calcium, with transient receptor potential (TRP) channels playing an integral role. This study determines the distribution and role of TRP canonical type-3 (C3) channels in the control of endothelium-derived hyperpolarization (EDH)-mediated vasodilator tone in rat mesenteric artery.

Methods and Results. TRPC3 antibody specificity was verified using rat tissue, HEK-293 cells stably transfected with mouse TRPC3 cDNA, and TRPC3 knock-out mouse tissue using Western blotting, confocal and ultrastructural immunohistochemistry. TRPC3-Pyr3 (ethyl-1-(4-(2,3,3-trichloroacrylamide)phenyl)-5-(trifluoromethyl)-1H-pyrazole-4-carboxylate) specificity was verified using patch clamp of mouse mesenteric artery endothelial and TRPC3-transfected HEK cells, and TRPC3 knock-out and wild-type mouse aortic endothelial cell calcium imaging and mesenteric artery pressure myography. TRPC3 distribution, expression and role in EDH-mediated function were examined in rat mesenteric artery using immunohistochemistry and Western blotting, and pressure myography and endothelial cell membrane potential recordings. In rat mesenteric artery, TRPC3 was diffusely distributed in endothelium, with ~5-fold higher expression at potential myoendothelial microdomain contact sites, and immunoelectron microscopy confirmed TRPC3 at these sites. Western blotting and endothelial damage confirmed primary endothelial TRPC3 expression. In rat mesenteric artery endothelial cells, Pyr3 inhibited hyperpolarization generation; and with individual SK_{Ca} (apamin) or IK_{Ca} (TRAM-34) block, Pyr3 abolished the residual respective IK_{Ca} and SK_{Ca}-dependent EDH-mediated vasodilation.

Conclusion. The spatial localization of TRPC3 and associated channels, receptors and calcium stores are integral for myoendothelial microdomain function. TRPC3 facilitate endothelial SK_{Ca} and IK_{Ca} activation, as key components of EDH-mediated vasodilator activity and for regulating mesenteric artery tone.

Keywords: endothelium, calcium channel, potassium channel, signalling microdomain, smooth muscle, vasodilation.

1. Introduction

The pathways that underlie endothelium-dependent vasodilation due to endothelium-derived hyperpolarization (EDH), are a topic of ongoing debate.[1,2] The specific mechanisms underlying EDH vary within and between vascular beds and in disease, where alterations represent potential therapeutic targets for correction.[3] In rat mesenteric artery, mechanisms intimately linked with EDH occur at specialized myoendothelial microdomain contact sites,[4-7] where localized gap junction connexins (Cxs)37 and 40, intermediate conductance calcium-activated potassium channels (IK_{Ca}), and endothelial endoplasmic reticulum (ER) inositol 1,4,5-trisphosphate receptors (IP_3R) are present.[5,7,8] Calcium influx across the membrane and Ca^{2+} release from stores underlie EDH generation.[9] Whilst EDH-related IP_3R-mediated calcium release[9,10] is the likely source of calcium for endothelial IK_{Ca} activation,[7] the source of calcium underlying small (S)K_{Ca}-related EDH activity is less well characterized, but is also likely to involve an IP_3R-dependent mechanism, perhaps via a pathway distinct to that associated with IK_{Ca}.

From a functional perspective, myoendothelial gap junction Cxs permit the direct transfer of an EDH current to the smooth muscle.[3,7,11] In addition, in rat mesenteric artery, IK_{Ca}-dependent K^+ release into the highly localized (<~30 nm) myoendothelial space between endothelial and smooth muscle cells facilitates diffusion-mediated signalling,[5-7] and separately or synergistically, activation of low level endothelial cell membrane SK_{Ca} and IK_{Ca}[8] may also contribute to EDH via their release of diffusible K^+ as a 'cloud' across the ~1 □m wide internal elastic lamina (IEL) 'space'.[12] Collectively, in the rat mesenteric artery, the SK_{Ca} and IK_{Ca}-dependent K^+ release activates adjacent smooth muscle Na-K-ATPase,[6,13] with the K^+ outflow also interacting with closely associated inward rectifying potassium channels (K_{ir}) on endothelial projections,[6,13] with some activity also potentially occurring at more diffusely distributed K_{ir} on the endothelial cell membrane. The net result of myoendothelial gap junction and K^+-mediated signalling is

hyperpolarization of the adjacent smooth muscle, closure of smooth muscle voltage-dependent calcium channels, inhibition of phospholipase C (PLC[14]) and vessel relaxation. In theory, there may be three types of myoendothelial signalling microdomains in the rat mesenteric artery; (1) those that facilitate current transfer (as myoendothelial gap junction/Cx-based sites only), (2), K^+-mediated signalling alone (as IK_{Ca}-IP_3R and / or SK_{Ca} based sites), or (3), a combination of these two mechanisms. Regardless, a regenerative mechanism of refilling of the localized ER calcium store is necessary at specialized myoendothelial microdomain sites to maintain the local functional mechanisms involved in EDH generation.

Transient receptor potential (TRP) channels are a family of generally non-selective cation channels that are activated and regulated by a wide variety of stimuli[15-18] and play significant roles in cellular calcium homeostasis. A role for several TRP channel subtypes in vascular function has been suggested[15,17-19] and in vascular EDH-type function, these include TRP ankyrin type 1 (A1[20,21]), TRP canonical type 3 (C3[22,23]), TRP vanilloid type 3 (V3[21]) and TRPV4.[24-26] In rat cerebral artery, TRPA1 has been suggested to play a role in myoendothelial signalling,[20] with a similar role being proposed for TRPC3 in co-cultured mouse aortic endothelial and smooth muscle cells.[22] In rat cerebral artery TRPV3 has also been suggested to facilitate endothelial cell calcium influx for EDH-type vasodilator activity.[21] In a similar manner, calcium entry through endothelial TRPV4 channels has been reported to trigger nitric oxide (NO)-dependent relaxation in rat carotid artery, and NO- and EDH-type relaxation in rat gracilis muscle arterioles.[25] A role for TRPV4 has also been suggested in EDH-type relaxation in rat cerebral artery;[24] with a potential role for such channels in NO- and EDH-type relaxation in mouse mesenteric artery.[26] However, no direct relationship with myoendothelial microdomain activity was demonstrated in the above endothelial TRPV3 and 4 studies.

The basis for investigating the potential role of TRPC3 in rat mesenteric artery comes from the suggestion that TRPC3 are present in close proximity to IP_3R[22] at myoendothelial contact sites in co-cultured mouse aortic endothelial and smooth muscle cells. An interactive association of TRPC3 and IP_3Rs has also been described in isolated uterine artery endothelial cells,[23] although whether this association occurred at myoendothelial microdomains in intact arteries was not clarified. Regardless, direct interaction of TRPC3 and IP_3R would be predicted to facilitate calcium entry at microdomain sites.

The present study determines the distribution and role of TRPC3 in the rat mesenteric artery; with the hypothesis that such channels are present at microdomains to facilitate ER calcium influx that underlies IK_{Ca} and SK_{Ca} activation and endothelial cell hyperpolarization, as an essential component of EDH-mediated vasodilation.

2. Methods

2.1 Animals and tissue

Adult male Sprague Dawley rats were anaesthetised with sodium pentathol (100 mg/kg; ip), and ~300 μm diameter 1st-3rd order mesenteric arteries dissected in Krebs' solution containing (in mM): 112 NaCl, 25 $NaHCO_3$, 4.7 KCl, 1.2 $MgSO_4.7H_2O$, 0.7 KH_2PO_4, 10 HEPES, 11.6 glucose, 2.5 $CaCl_2.2H_2O$; pH 7.3. Male 8-10 week old TRPC3 KO mice[27] generated on a 129SvEv/C57BL/6J mixed background and age-matched littermate WT controls were anaesthetized with isofluorane and the aorta dissected in Hank's balanced salt solution for imaging studies. Rat liver, and mouse liver, aorta and mesenteric arteries were also dissected from anaesthetized (sodium pentathol; 100 mg/kg; ip) animals for reagent characterization studies.

All procedures conform with the Guide for the Care and Use of Laboratory Animals published by the US National Institutes of Health (NIH Publication No. 85-23, revised 1996), and were approved by the Animal Ethics Committees of the University of New South Wales

(09/43B), Monash University (SOBSA/P/2007/100), and Baylor College of Medicine (AN-4366). Respiration rate and tactile responses were monitored to indicate adequacy of anaesthesia.

2.2 Reagent characterization

TRPC3 antibody specificity was determined by immunohistochemistry using stably transfected HEK-293 cells expressing mouse TRPC3 (Supplementary material online, *Figure S1A-C*), and by confocal immunohistochemistry (Supplementary material online, *Figures S1D-I, S2A*) and Western blotting using extracts of tissues from rat (Supplementary material online, *Figure S3*).

The specificity of the putative TRPC3 blocker Pyr3 (ethyl-1-(4-(2,3,3-trichloroacrylamide)phenyl)-5-(trifluoromethyl)-1H-pyrazole-4-carboxylate) was validated by pressure myography in mesenteric artery from KO and WT mice, patch clamp using freshly isolated mouse mesenteric artery endothelial cells (Supplementary material online, *Figure S4*) and transfected HEK cells expressing TRPC3 (Supplementary material online, *Figure S5*) and by calcium imaging using aortic endothelial cells obtained from KO and WT mice (Supplementary material online, *Figure S2B*).

Full methods, including patch clamp and calcium imaging used for reagent characterization; as well as statistics, drug and reagent details are available online as Supplementary Data. Primary antibody and primer characteristics are detailed in Supplementary material online, *Tables S1*, *S2*.

2.3 Rat mesenteric artery TRPC3

The characteristics of TRPC3 channels in adult male Sprague Dawley rat mesenteric artery were determined using confocal and ultrastructural immunohistochemistry, Western blotting and pressure myography and endothelial cell membrane potential recordings (*Figures 1-2*).

2.3.1 Histology

The distribution of TRPC3 was examined in rat mesenteric artery, and KO and WT mouse aorta and mesenteric artery, using conventional confocal immunohistochemistry as previously described.[4,8] The distribution of von Willebrand Factor (vWF) was examined and arteries in which the endothelium had been disrupted compared to intact artery, with methods as previously described.[4,8,28]

2.3.2 Western blotting

The specificity of TRPC3 antibody and characteristics of TRPC3 channels in adult male Sprague Dawley rat mesenteric artery were determined using Western blotting. Rat mesenteric arteries and liver, and mouse liver were rapidly frozen, and stored in liquid nitrogen, with Western blotting conducted with controls, as previously described.[13,29] Of note, to verify potential endothelial or smooth muscle cell TRPC3 expression, samples were prepared for Western blotting using rat mesenteric artery from which the endothelium had been disrupted.

2.3.3 TRPC3 and EDH-mediated vasodilation - pressure myography

The characteristics of TRPC3 channels in adult male Sprague Dawley rat and mouse mesenteric artery were determined using pressure myography. Freshly dissected rat (internal diameter in 0 mM calcium, 287 ± 6 μm; n=15) and mouse mesenteric arteries (internal diameter in 0 mM

calcium, control, 175 ± 8 µm; *n*=4; TRPC3 KO, 167 ± 8 µm; *n*=6) were cannulated in a pressure myograph and continuously superfused with Krebs' solution (37°C) at a rate of 3 ml/minute, bubbled with 5% CO_2-95% N_2. Arteries were pressurized to 80 mmHg with incremental increases over 80 minutes. Vessels were initially pre-constricted with superfused PE (1 □M; to 80% of maximum constriction; including with equal levels of preconstriction in the presence of Pyr3, TRAM and apamin), which was present in all experiments. Endothelium-dependent vasodilation in rat mesenteric arteries was evoked with increasing concentrations of ACh (1 nM-30 □M) added cumulatively to the bath; whilst the response in mouse mesenteric artery was evoked using the PAR-2 agonist, SLIGRL at 10□M.[30]

Experiments were conducted in the presence of N^{ω}-nitro-L-arginine methyl ester (L-NAME; 100 □M; NO synthase blocker), ODQ (1H-[1,2,4] oxadiazolo-[4,3-a]quinoxalin-1-one]; 10 □M; sGC blocker), and indomethacin (10 □M; cyclooxygenase blocker), as well as the putative TRPC3 blocker Pyr3(1 □M for 20 minutes[31]), apamin (15 minutes; 100 nM), and / or 1-[(2-chlorophenyl)diphenylmethyl]-1H-pyrazole (TRAM-34; 30 minutes; 1 □M); the latter two agents as defining blockers of EDH.[1,12,32]; prior to addition of ACh or SLIGRL. Additional experiments on rat mesenteric artery were also performed in the absence of L-NAME, ODQ and indomethacin. Artery diameter changes are expressed as a percentage of the maximal dilation achieved by replacing the control Krebs' solution with calcium-free Krebs' solution at the end of the experiment.

2.3.4 TRPC3 and EDH - sharp electrode electrophysiology

The characteristics of TRPC3 channels in adult male Sprague Dawley rat mesenteric artery were determined using endothelial cell membrane potential recordings. Freshly dissected rat mesenteric arteries were cut along the longitudinal axis and pinned endothelium uppermost to the base of a

recording chamber and continuously superfused as described previously.[4] L-NAME (200 □M) and indomethacin (1 □M) were present in all experiments. The membrane potential of endothelial cells was recorded using intracellular glass microelectrodes containing 1 M KCl (100-140 MΩ resistance) and the tips were filled with Lucifer Yellow CH to allow unequivocal identification of every impaled cell.[4] Endothelial cells were stimulated with 1 μM ACh for 1 minute. Responses were recorded in the absence (control) and presence of Pyr3 (1 μM), TRAM 34 (5 μM) and apamin (100 nM). Responses recorded in the presence of blockers were expressed as a percent of the control response in L-NAME and indomethacin.

3. Results

3.1 Reagent characterization

Specificity of the TRPC3 antibody was confirmed using confocal immunohistochemistry. TRPC3 was absent in both cell layers of TRPC3 KO mouse mesenteric artery (Supplementary material online, *Figure S1H, I*). In WT mesenteric artery TRPC3 was present in the endothelium, but there was an apparent absence in the smooth muscle (Supplementary material online, *Figure S1D-G*). Under equivalent conditions, TRPC3 was detected in the endothelium and smooth muscle of WT aorta (Supplementary material online, *Figure S2A*).

Additional specificity data for Pyr3 and the TRPC3 antibody are detailed in the Supplementary material online, Results and Discussion, and *Figures S1-S5.*

3.2 Mesenteric artery

3.2.1 TRPC3 protein localization and expression

The distribution of TRPC3 in rat mesenteric artery was determined using confocal immunohistochemistry of whole mount tissue (*Figure 1A-C*), as well as high resolution

ultrastructural immunolocalization (*Figure 1D-F*). Semi-quantitative mean fluorescence density of TRPC3 over the endothelial cell membrane, exclusive of IEL hole sites, was 2558 ± 115, compared to 13827 ± 788 arbitrary units for IEL holes sites exhibiting densities of TRPC3 labelling (*Figure 1B*). Thus, TRPC3 was present at a low level over the endothelial cell membrane at non-IEL hole sites, with a >5-fold higher fluorescence density at ~73% of IEL hole sites (*Figure 1A-D*; *Tables 1, 2*). The comparative frequency of TRPC3 at the IEL sites was ~3-fold higher than that of myoendothelial gap junctions, which were present at ~23% of IEL holes sites (*Tables 1, 2*). Confocal fluorescence density of TRPC3 labelled rat mesenteric artery smooth muscle was not significantly different from that of the negatively labeled TRPC3 knock-out (KO) mouse mesenteric artery smooth muscle (1187 ± 27, compared to 1225 ± 10 arbitrary units; $P<0.05$; compare *Figures 1C*, inset and Supplementary material online, *Figure S1I*, respectively). Ultrastructural immunohistochemistry confirmed TRPC3 expression at regions of close association of endothelial and smooth muscle cells of <30 nm (*Figure 1D-F*), as potential myoendothelial microdomain sites, as well as at the endothelial, but not the smooth muscle cell membrane and cytoplasm. TRPC3 was also expressed in the perivascular nerve plexus (*Figure 1B*, inset).

Rat mesenteric artery TRPC3 protein expression was confirmed by Western blotting, which recognized the monoglycosylated and complex forms of TRPC3 protein as faint bands at ~120 kDa, and >~220 kDa, respectively (*Figure 1G, H*; Supplementary material online, *Figure S3C,D*); as well as a band at ~60 kDa (*Figure 1G*; Supplementary material online, *Figure S3C,D*), which is a likely breakdown product of the TRPC3 protein. Each of these bands was abolished by peptide block of the primary antibody. To verify potential endothelial or smooth muscle cell TRPC3 expression, Western blots were run on endothelium-disrupted, compared to intact mesenteric artery. TRPC3 signal at ~120 and >~220 kDa from intact vessels was ~2-fold

higher than from endothelium-disrupted vessels (*Figure 1G, H*), with the ~60 kDa band being reduced in a similar manner (*Figure 1G*). Endothelium-disruption of samples of the same vessel segments as used in the endothelium-disrupted Western blot experiments, was confirmed with von Willebrand Factor (vWF) immunohistochemistry (*Figure 1G*, lower panels).

3.2.2 TRPC3 and EDH-mediated vasodilation - pressure myography

In rat mesenteric arteries, in the presence of L-NAME, ODQ, and indomethacin, acetylcholine (ACh)-induced vasodilation was significantly attenuated and blocked by respective 0.3 and 1 μM Pyr3 application (*Figure 2A*; *Table 3*). In the absence of L-NAME, ODQ and indomethacin, maximum ACh-induced dilation was unaffected, although the sensitivity to ACh was increased (Supplementary material online, *Figure S6*). Further, the absence of L-NAME, ODQ and indomethacin had no effect on the maximum dilation in the presence of 1 μM Pyr3 (Supplementary material online, *Figure S6*). Higher concentrations of Pyr3 (3 and 10 μM) were found to block phenylephrine (PE)-induced constriction (*n*=3, each; data not shown), and thus 1 μM was used in subsequent experiments, for specific Pyr3 block. ACh-induced vasodilation was significantly attenuated by the SK_{Ca} blocker, apamin (100 nM), and abolished with the additional application of Pyr3 (1 μM; *Figure 2B; Table 3*) or the IK_{Ca} blocker, TRAM-34 (1 μM; *Table 3*). In a similar manner, ACh-induced vasodilation was significantly attenuated by TRAM-34, and abolished with the addition of Pyr3 (*Figure 2C; Table 3*). Thus, with individual SK_{Ca} or IK_{Ca} block, Pyr3 blocked the respective residual K_{Ca}-mediated components of EDH-mediated vasodilation.

3.2.3 Sharp electrode electrophysiology - endothelial cell membrane potential

In the presence of L-NAME and indomethacin, ACh (1 μM) evoked a hyperpolarization of 23 ± 1 mV (*n*=6) in rat mesenteric artery endothelial cells, with Pyr3 (1 μM) significantly reducing the hyperpolarization amplitude (*Figure 2D, E*). In the presence of Pyr3, the hyperpolarization had a complex nature consisting of an initial rapid component of 13 ± 2 mV (*n*=6, *P*<0.05, compared with control; *Figure 2D*; C1 in *Figure 2E*) followed by a second slower component of 8 ± 3 mV (*n*=6, *P*<0.05, compared with control; *Figure 2D*; C2 in *Figure 2E*). Both components of this remaining hyperpolarization were abolished by the combination of TRAM 34 and apamin (*Figure 2D, E*).

4. Discussion

The present anatomical and functional data support a link between TRPC3 channels, and the K_{Ca} channel-mediated endothelial vasodilator function associated with the EDH mechanism in the rat mesenteric artery. TRPC3 likely facilitate calcium entry for close spatially associated IP_3R-dependent ER calcium store refilling;[7,9,10] and/or direct activation of SK_{Ca} and IK_{Ca}. Support for such a role of TRPC3 is illustrated in the present study by coincident TRPC3 and IK_{Ca} localization at a higher density at a proportion of IEL hole sites, as well as at the endothelial cell surface, where lower level SK_{Ca} and IK_{Ca} occur.[6,8,13] Similar spatial localization of ER-IP_3R occurs near the cell membrane in the subplasmalemmal compartment,[33] with higher level localization at IEL-hole sites[7,34] (summarized in *Figure 3*; see also Supplementary material online, *Figure S7*). Further, functional Pyr3-mediated TRPC3 block selectively abolishes the remaining respective SK_{Ca}- and IK_{Ca}-mediated EDH activity. Collectively, these data support the presence of a functional signalling microdomain which is critical for EDH activity in the rat mesenteric artery.

A functional and spatial association between TRPC3, IP_3R and K_{Ca} exists in a variety of cell types. For example, a functional interaction of IP_3R and TRPC3 has been proposed in human embryonic kidney (HEK)-293 cells,[35] cultured bovine pulmonary artery endothelial[36] and passage 3-4 bovine uterine artery endothelial cells;[23] the latter being suggested to relate to NO-mediated activity.[37] Further demonstration of such a relationship has also been shown in rat cerebral artery, and in isolated smooth muscle cells of these arteries;[38] as well as in isolated rabbit coronary artery smooth muscle cells.[39] Similar reports of a functional interaction of IP_3R and large conductance K_{Ca} have also been suggested in isolated basilar artery smooth muscle cells,[40] and in cultured murine pancreatic β-cells;[41] whilst IP_3R and IK_{Ca} have been reported to functionally interact in isolated guinea pig gastric smooth muscle cells.[42] Thus, the precedent for functional interaction of TRPC3, IP_3R and K_{Ca} exists, supporting the potential spatial-related functional activity of these channels and receptors in myoendothelial signalling in the rat mesenteric artery.

The present data show that in the mesenteric artery of adult male rats, TRPC3 is expressed in endothelial cells. Indeed, given that the endothelium constitutes a relatively small mass of the vessel wall compared to the smooth muscle (<~10%; see *Figure 2* in[43] and *Figure 1A* in,[13] for example), that TRPC3 expression is reduced by >50% with endothelial removal, and that TRPC3 is expressed in the perivascular nerve plexus (*Figure 1B*, inset), any smooth muscle TRPC3 expression in the intact rat mesenteric artery is negligible.

In rat mesenteric artery, 0.3 to 1 μM Pyr3 significantly attenuates EDH-mediated vasodilation, with this activity being verified in mesenteric artery from KO and WT mice. At these concentrations the actions of Pyr3 were selective for EDH-mediated vasodilation (see also Supplementary material online, *Figure S6*) and did not influence the level of underlying vasoconstriction, with patch clamp data supporting a lack of direct Pyr3 effect on SK_{Ca} or IK_{Ca} (*Figure S4*). Furthermore, when either SK_{Ca} or IK_{Ca} were blocked, subsequent exposure to Pyr3

blocked the residual EDH-mediated vasodilator activity. This indicates that TRPC3 channels are integral to the function of SK_{Ca} and IK_{Ca}, and thus underpin key aspects of EDH activity in rat mesenteric artery. Consistent with this, Pyr3 inhibited the generation of hyperpolarization in mesenteric endothelial cells which is the initial critical step for EDH activity. The transformation of the endothelial cell hyperpolarization into a complex multi-component response in the presence of Pyr3 is reminiscent of changes seen in EDH-mediated smooth muscle responses following inhibition of the different sources of Ca^{2+} in rat mesenteric arteries.[9] Thus, the actions of Pyr3 may reflect inhibition of Ca^{2+} influx pathways necessary for ER Ca^{2+} store refilling and for direct activation of SK_{Ca} and IK_{Ca} in rat mesenteric artery (*Figure 3*). Notably, EDH actions extend from transient to more tonic effects on blood flow regulation *in vivo*,[44-46] and the relative contribution of different EDH mechanisms to vasodilation can vary between isometric versus isobaric conditions and *in vivo*.[47] The role of TRPC3 in the generation of EDH under *in vivo* conditions will need to be elucidated in future studies.

The present data lend further support to the concept that there is heterogeneity in EDH-related myoendothelial signalling mechanisms in the rat mesenteric artery (*Figure 3;* see also[4-10,13,34,48,49]). Based on present and previously published data from this vessel on the function and distribution of TRPC3, SK_{Ca}, IK_{Ca}, IP_3R and myoendothelial gap junctions, three potential signalling pathways for EDH-related activity at myoendothelial contact sites exist in the normal rat mesenteric artery, as: 1. TRPC3-IK_{Ca}-IP_3R functional microdomains at ~70-80% of IEL hole sites, of which ~25-30% are also associated with myoendothelial gap junction sites (*Table 2*); these latter sites also facilitating, 2. Cx-mediated transfer of current; with mechanism 3. a combination of 1. and 2. Indeed, these mechanisms may operate independently or in synergy; as suggested for similar mechanisms in the human mesenteric[50] and saphenous artery of the obese rat.[29]

This study characterized the selectivity and potency of a putative TRPC3 blocker, Pyr3,[31] in rat mesenteric artery, with additional characterization of the agent being carried out in transfected HEK cells expressing murine TRPC3 and in WT and KO mouse tissues. Pyr3 was found to attenuate the carbachol (CCh)-induced inward current in transfected HEK cells expressing TRPC3 (Supplementary material online, *Figure S5*), as well as the CCh-induced calcium influx component in WT, but not KO-derived aortic endothelial cells (Supplementary material online, *Figure S2B*); as well the ATP-induced K^+ current in mouse mesenteric artery endothelial cells (Supplementary material online, *Figure S4*). Interestingly, the Pyr3 response in the WT cell line does not completely mimic that in the KO cell line (Supplementary material online, *Figure S2B*). The slight attenuation of the response in KO cells was limited to the early phase of the calcium response, as typically associated with release from internal stores,[51] and suggests a degree of potential non-specific action at higher (10 μM) Pyr3 concentrations. Indeed, the concentration used in the present calcium imaging work is ~3-fold higher than the 3 μM full Pyr3 block previously reported using HEK cells transfected with murine TRPC3.[31]

The smooth muscle layer of the rat mesenteric artery is the site of action for the α-adrenergic agonist and vasoconstrictor, PE. The absence of TRPC3 at this site (see present data and[48]) and the block of PE-induced constriction by 3 and 10 μM Pyr3 observed in this study, suggests that Pyr3 may possess a non-specific action at these concentrations in the smooth muscle layer of intact vessels; consistent with the above potential early phase non-specific Pyr3 action on calcium in isolated endothelial cells. Together, these findings suggest that Pyr3 is an effective inhibitor of TRPC3 channels, but at higher concentrations may have concentration-dependent non-selective effects possibly related to inhibition of calcium release from internal stores.

Concluding remarks

TPRC3 channel localization and function in rat mesenteric artery is consistent with their role at myoendothelial signalling sites associated with endothelial cell calcium dynamics and K_{Ca}-dependent EDH. In this role, TRPC3 channels likely promote activation of endothelial SK_{Ca} and IK_{Ca} through providing calcium directly to the channels and/or facilitating refilling of the IP_3R-mediated ER calcium stores (*Figure 3;* see also[4-10,13,34,48,49]). Thus, TRPC3 have a fundamental role in EDH-mediated vasodilation and thus in the regulation of vascular tone in rat mesenteric artery.

Supplementary material

Supplementary material is available at *Cardiovascular Research* online.

Conflict of interest: none.

Funding

This work was supported by grants from the National Health and Medical Research Council of Australia [ID401112, 455243 to S.L.S.; 510202 to P.B.; 546087 to M.T. and S.L.S.], the Australian Research Council [DP1097202 to G.D.H.] and the National Institutes of Health [project Z01-ES-101684 to L.B.; R01 HL088435 to S.P.M.].

References

1. Sandow SL, Tare M. C-type natriuretic peptide: a new endothelium-derived hyperpolarizing factor? *Trends Pharmacol Sci* 2007;**28**:61-67.
2. Kohler R, Hoyer J. The endothelium-derived hyperpolarizing factor: insights from genetic animal models. *Kidney Int* 2007;**72**:145-150.
3. Feletou M. Calcium-activated potassium channels and endothelial dysfunction: therapeutic options? *Br J Pharmacol* 2009;**156**:545-562.
4. Sandow SL, Tare M, Coleman HA, Hill CE, Parkington HC. Involvement of myoendothelial gap junctions in the actions of EDHF. *Circ Res* 2002;**90**:1108-1113.
5. Mather S, Dora KA, Sandow SL, Winter P, Garland CJ. Rapid endothelial cell-selective loading of connexin 40 antibody blocks EDHF dilation in rat small mesenteric arteries. *Circ Res* 2005;**97**:399-407.
6. Dora KA, Gallagher NT, McNeish A, Garland CJ. Modulation of endothelial cell $K_{Ca}3.1$ channels during EDHF signaling in mesenteric resistance arteries. *Circ Res* 2008;**102**:1247-1255.
7. Sandow SL, Haddock RE, Hill CE, Chadha PE, Kerr PM, Welsh DG *et al.* What's where and why at a vascular myoendothelial microdomain signaling complex? *Clin Exp Pharmacol Physiol* 2009;**36**:67-76.
8. Sandow SL, Neylon CB, Chen MX, Garland CJ. Spatial separation of endothelial small- and intermediate-conductance calcium-activated potassium channels (K_{Ca}) and connexins: possible relationship to vasodilator function? *J Anat* 2006;**209**:689-698.
9. Fukao M, Hattori Y, Kanno M, Sakuma I, Kitabatake A. Sources of Ca^{2+} in relation to generation of acetylcholine-induced endothelium-dependent hyperpolarization in rat mesenteric artery. *Br J Pharmacol* 1997;**120**:1328-1334.

10. Cao YX, Zheng JP, He JY, Li J, Xu CB, Edvinsson L. Induces vasodilatation of rat mesenteric artery *in vitro* mainly by inhibiting receptor-mediated Ca^{2+}-influx and Ca^{2+}-release. *Arch Pharmacol Res* 2005;**28**:709-715.

11. de Wit C, Griffith TM. Connexins and gap junctions in the EDHF phenomenon and conducted vasomotor responses. *Pflugers Arch* 2010;**459**:897-914.

12. Busse R, Edwards G, Feletou M, Fleming I, Vanhoutte PM, Weston AH. EDHF: bringing the concepts together. *Trends Pharmacol Sci* 2002;**23**:374-380.

13. Haddock RE, Grayson TH, Morris MJ, Howitt L, Chadha PS, Sandow SL. Diet-induced obesity impairs endothelium-derived hyperpolarization via altered potassium channel signaling mechanisms. *PloS One* 2011;**6**:e16423.

14. Itoh T, Seki N, Suzuki S, Ito S, Kajikuri J, Kuriyama H. Membrane hyperpolarization inhibits agonist-induced synthesis of IP_3 in rabbit mesenteric artery. *J Physiol* 1992;**451**:307-328.

15. Brayden JE, Earley S, Nelson MT, Reading S. Transient receptor potential (TRP) channels, vascular tone and autoregulation of cerebral blood flow. *Clin Exp Pharmacol Physiol* 2008;**35**:1116-1120.

16. Abramowitz J, Birnbaumer L. Physiology and pathophysiology of canonical transient receptor potential channels. *FASEB J* 2009;**23**:297-328.

17. Vennekens R. Emerging concepts for the role of TRP channels in the cardiovascular system. *J Physiol* 2011;**589**:1527-1534.

18. Earley S, Brayden JE. Transient receptor potential channels and vascular function. *Clin Sci* 2010;**119**:19-36.

19. Yao X, Garland CJ. Recent developments in vascular endothelial cell transient receptor potential channels. *Circ Res* 2005;**97**:853-863.

20. Earley S, Gonzales AL, Crnich R. Endothelium-dependent cerebral artery dilation mediated by TRPA1 and Ca^{2+}-activated K^+ channels. *Circ Res* 2009;**104**:987-994.

21. Earley S, Gonzales AL, Garcia ZI. A dietary agonist of TRPV3 elicits endothelium-dependent vasodilation. *Mol Pharmacol* 2010;**77**:612-620.

22. Isakson BE, Duling BR. Organization of IP_3-R1 and TRPC3 at the myoendothelial junction may influence polarized calcium signaling. *Experimental Biology (Late Breaking Abstracts)* 2006:786.783.

23. Gifford SM, Yi FX, Bird IM. Pregnancy-enhanced store-operated Ca^{2+} channel function in uterine artery endothelial cells is associated with enhanced agonist-specific transient receptor potential channel 3-IP_3R2 interaction. *J Endocrinol* 2006;**190**:385-395.

24. Marrelli SP, O'Neil R G, Brown RC, Bryan RM, Jr. PLA_2 and TRPV4 channels regulate endothelial calcium in cerebral arteries. *Am J Physiol* 2007;**292**:H1390-1397.

25. Kohler R, Heyken WT, Heinau P, Schubert R, Si H, Kacik M *et al.* Evidence for a functional role of endothelial transient receptor potential V4 in shear stress-induced vasodilatation. *Arterioscler Thromb Vasc Biol* 2006;**26**:1495-1502.

26. Mendoza SA, Fang J, Gutterman DD, Wilcox DA, Bubolz AH, Li R *et al.* TRPV4-mediated endothelial Ca^{2+} influx and vasodilation in response to shear stress. *Am J Physiol* 2010;**298**:H466-476.

27. Hartmann J, Dragicevic E, Adelsberger H, Henning HA, Sumser M, Abramowitz J *et al.* TRPC3 channels are required for synaptic transmission and motor coordination. *Neuron* 2008;**59**:392-398.

28. Haddock RE, Grayson TH, Brackenbury TD, Meaney KR, Neylon CB, Sandow SL *et al.* Endothelial coordination of cerebral vasomotion via myoendothelial gap junctions containing connexins37 and 40. *Am J Physiol* 2006;**291**:H2047-H2056.

29. Chadha PS, Haddock RE, Howitt L, Morris MJ, Murphy TV, Grayson TH *et al.* Obesity upregulates IK_{Ca} and myoendothelial gap junctions to maintain endothelial vasodilator function. *J Pharmacol Exp Ther* 2010;**335**:284-293.

30. Beleznai T, Takano H, Hamill C, Yarova P, Douglas G, Channon K *et al.* Enhanced K^+-channel-mediated endothelium-dependent local and conducted dilation of small mesenteric arteries from ApoE-/- mice. *Cardiovasc Res* 2011;**92**:199-208.

31. Kiyonaka S, Kato K, Nishida M, Mio K, Numaga T, Sawaguchi Y *et al.* Selective and direct inhibition of TRPC3 channels underlies biological activities of a pyrazole compound. *Proc Natl Acad Sci USA* 2009;**106**:5400-5405.

32. McGuire JJ, Ding H, Triggle CR. Endothelium-derived relaxing factors: a focus on endothelium-derived hyperpolarizing factor(s). *Can J Physiol Pharmacol* 2001;**79**:443-470.

33. Isshiki M, Mutoh A, Fujita T. Subcortical Ca^{2+} waves sneaking under the plasma membrane in endothelial cells. *Circ Res* 2004;**95**:e11-21.

34. Sandow SL, Senadheera S, Bertrand PP, Murphy TV, Tare M. Myoendothelial contacts, gap junctions and microdomains: anatomical links to function? *Microcirculation* 2012;**19**:doi:10.1111/j.1549-8719.2011.00146.x.

35. Boulay G, Brown DM, Qin N, Jiang M, Dietrich A, Zhu MX *et al.* Modulation of Ca^{2+} entry by polypeptides of the inositol 1,4, 5-trisphosphate receptor (IP_3R) that bind transient receptor potential (TRP): evidence for roles of TRP and IP_3R in store depletion-activated Ca^{2+} entry. *Proc Natl Acad Sci USA* 1999;**96**:14955-14960.

36. Kamouchi M, Philipp S, Flockerzi V, Wissenbach U, Mamin A, Raeymaekers L *et al.* Properties of heterologously expressed hTRP3 channels in bovine pulmonary artery endothelial cells. *J Physiol* 1999;**518**:345-358.

37. Yi FX, Boeldt DS, Gifford SM, Sullivan JA, Grummer MA, Magness RR *et al.* Pregnancy enhances sustained Ca^{2+} bursts and endothelial nitric oxide synthase activation in ovine uterine artery endothelial cells through increased connexin 43 function. *Biol Reprod* 2010;**82**:66-75.

38. Adebiyi A, Zhao G, Narayanan D, Thomas CM, Bannister JP, Jaggar JH. Isoform-selective physical coupling of TRPC3 channels to IP_3R in smooth muscle cells regulates arterial contractility. *Circ Res* 2010;**106**:1603-1612.

39. Peppiatt-Wildman CM, Albert AP, Saleh SN, Large WA. Endothelin-1 activates a Ca2+-permeable cation channel with TRPC3 and TRPC7 properties in rabbit coronary artery myocytes. *J Physiol* 2007;**580**:755-764.

40. Kim CJ, Weir BK, Macdonald RL, Zhang H. Erythrocyte lysate releases Ca^{2+} from IP_3-sensitive stores and activates Ca^{2+}-dependent K^+ channels in rat basilar smooth muscle cells. *Neurol Res* 1998;**20**:23-30.

41. Ammala C, Larsson O, Berggren PO, Bokvist K, Juntti-Berggren L, Kindmark H *et al.* Inositol trisphosphate-dependent periodic activation of a Ca^{2+}-activated K^+ conductance in glucose-stimulated pancreatic beta-cells. *Nature* 1991;**353**:849-852.

42. Yang M, Li XL, Xu HY, Sun JB, Mei B, Zheng HF *et al.* Role of arachidonic acid in hyposmotic membrane stretch-induced increase in calcium-activated potassium currents in gastric myocytes. *Acta Pharmacol Sin* 2005;**26**:1233-1242.

43. Sandow SL, Hill CE. The incidence of myoendothelial gap junctions in the proximal and distal mesenteric arteries of the rat is suggestive of a role in EDHF-mediated responses. *Circ Res* 2000;**86**:341-346.

44. Taylor MS, Bonev AD, Gross TP, Eckman DM, Brayden JE, Bond CT *et al.* Altered expression of small-conductance Ca^{2+}-activated K^+ (SK3) channels modulates arterial tone and blood pressure. *Circ Res* 2003;**93**:124-131.

45. Si H, Heyken WT, Wolfle SE, Tysiac M, Schubert R, Grgic I *et al.* Impaired EDHF-mediated dilations and increased blood pressure in mice deficient of the intermediate-conductance Ca^{2+}-activated K^+ channel. *Circ Res* 2006;**99**:537-544.

46. Milkau M, Kohler R, de Wit C. Crucial importance of the endothelial K^+ channel SK3 and connexin40 in arteriolar dilations during skeletal muscle contraction. *FASEB J* 2010;**24**:3572-3579.

47. Boettcher M, de Wit C. Distinct endothelium-derived hyperpolarizing factors emerge *in vitro* and *in vivo* and are mediated in part via connexin 40-dependent myoendothelial coupling. *Hypertension* 2011;**57**:802-808.

48. Hill AJ, Hinton JM, Cheng H, Gao Z, Bates DO, Hancox JC *et al.* A TRPC-like non-selective cation current activated by α1-adrenoceptors in rat mesenteric artery smooth muscle cells. *Cell Calcium* 2006;**40**:29-40.

49. Sandow SL, Gzik DJ, Lee RMKW. Arterial internal elastic lamina holes: relationship to function? *J Anat* 2009;**214**:258-266.

50. Chadha PS, Lu L, Rikard-Bell M, Senadheera S, Howitt L, Bertrand RL *et al.* Endothelium-dependent vasodilation in human mesenteric artery is primarily mediated by myoendothelial gap junctions, IK_{Ca} and NO. *J Pharmacol Exp Ther* 2011;**336**:701-708.

51. Adams DJ, Barakeh J, Laskey R, Van Breemen C. Ion channels and regulation of intracellular calcium in vascular endothelial cells. *FASEB J* 1989;**3**:2389-2400.

52. Milner P, Belai A, Tomlinson A, Hoyle CH, Sarner S, Burnstock G. Effects of long-term laxative treatment on neuropeptides in rat mesenteric vessels and caecum. *J Pharm Pharmacol* 1992;**44**:777-779.

53. Goel M, Sinkins WG, Schilling WP. Selective association of TRPC channel subunits in rat brain synaptosomes. *J Biol Chem* 2002;**277**:48303-48310.

54. Dietrich A, Mederos y Schnitzler M, Emmel J, Kalwa H, Hofmann T, Gudermann T. N-linked protein glycosylation is a major determinant for basal TRPC3 and TRPC6 channel activity. *J Biol Chem* 2003;**278**:47842-47852.

55. Hill CE. Long distance conduction of vasodilation: A passive or regenerative process? *Microcirculation* 2012;**19**:In Press. doi:10.1111/j.1549-8719.2012.00169.x

Figure legends

Figure 1 TRPC3 localization and expression in rat mesenteric artery. Localized holes (dark spots; examples with arrows, *A*), are present in the internal elastic lamina (IEL; *A*) between the vascular endothelium and smooth muscle. TRPC3 presence in endothelial cells (EC; *B,C*) and apparent absence in smooth muscle cells (*C*, inset) was demonstrated using TRPC3 antibody batches AN-02, 03 and 07 (Supplementary material online, *Table S1*; AN-07, as example used here). Low level diffuse TRPC3 is localized to the endothelial membrane (*B*), whilst overlay of IEL and TRPC3 label (*C*) shows strong TRPC3 expression at a proportion of IEL holes at the IEL-SM focal plane border (examples arrowed with asterisks; see also *Tables 1, 2*), as potential myoendothelial microdomain sites; noting that not all such sites have localized TRPC3 densities (example, arrow with no asterisk). Peptide block abolished staining (*A*, inset); with no labelling being present when incubated in secondary antibody alone (data not shown). Perivascular nerve labeling (compare morphology to[52]) acts as a positive control (*B*, inset, examples arrowed). TRPC3 antibody (AN-07) conjugated to 10 nm colloidal gold (*D-F*) confirms TRPC3 localization to myoendothelial contact regions (*F*, examples arrowed), as potential myoendothelial microdomain signalling sites, as well as at other sites within the endothelium (*B*, examples arrowed). Vessel region in panels A-C, correspond. Longitudinal vessel axis (*A-C*), left to right, *n*=6 and 3, each from a different animal (*A-C; D-F*, respectively). The characteristics of rat mesenteric artery TRPC3 and its primary endothelial expression were examined using Western blotting and TRPC3 antibody (ACC-016; AN-07 used here; Supplementary material online, *Table S1*). Monoglycosylated TRPC3 is present as a band at ~120 kDa (*G2*, box; +EC; see also[53]), whilst the band at >~220 kDa (*G1*, box; see also[54]) probably represents an undissociated aggregate of the TRPC3 tetrameric channel complex. TRPC3 expression was normalized to actin (at ~43 kDa; lower bands, *G*), with endothelial removal (-EC; *G*, upper right column) reducing TRPC3 expression at ~120 and >~220 kDa by ~2-fold each (*H*, upper and lower,

respectively; *P<0.05, significant; values being mean±SEM). Two lanes per artery were run with tissue from 3 different rats, 12 in total, with 20 µg of protein per lane being loaded. von Willebrand Factor (vWF) labelling verified endothelial removal in whole mount preparations (*G*, lower panels). Scale bars, 25 µm (*A-C,G*), 50 µm (*B*, inset), 5 µm (*D*), 2 µm (*E*), 1 µm (*F*).

Figure 2 TRPC3 in endothelium-dependent relaxation and endothelial cell hyperpolarization in rat mesenteric artery. In pressurized rat mesenteric arteries, relaxation to ACh (1 nM-100 µM) was examined in the presence and absence of Pyr3 (0.3 µM, *A*; 1 µM in *A-C*) with apamin (50 nM; *B*), or TRAM-34 (1 µM; *C*), or combined apamin and TRAM-34, to determine the relative contribution of TRPC3, SK_{Ca} and IK_{Ca}. L-NAME (100 µM), ODQ (10 µM) and indomethacin (10 µM) were present in all experiments. n=5-7 experiments, each from different animals; P<0.05 indicates difference in *pEC_{50}, or $^{\#}E_{max}$, relative to ACh control (see *Table 3* for drug characteristics). The endothelial cell hyperpolarization evoked by ACh (1 µM; 100%; n=6; *Ei*) in the presence of L-NAME (100 µM) and indomethacin (10 µM) was recorded in the presence of Pyr3 alone (1 µM; n=6; *Eii*), Pyr3 and TRAM-34 (5 µM; n=4; *Eiii*), and Pyr3, TRAM-34 and apamin (100 nM, n=4; *D, Eiv*). Example endothelial cell membrane potential recordings show hyperpolarization before and after the addition of Pyr3, TRAM-34 and apamin (*Eii-iv*). Pyr3 (1 µM) reduced the hyperpolarization to ACh (*D, Eii-iv*), with the remaining hyperpolarization having a complex nature (*D, Eii-iv*), consisting of an initial rapid component (*C1*, with arrow in *Eii,iii*) followed by a second slower component (*C2*, with arrow in *Eii,iii*). In the presence of all blockers, ACh evoked endothelial cell depolarization (*E*, far right) trace. Inset shows example of dye-filled endothelial cells (*Ea*, inset, arrow) indicates cell from which recording was made. Scale bar, 50 µm, with longitudinal vessel axis, left to right.

Figure 3 Vasodilator signalling mechanism at myoendothelial contact sites in rat mesenteric artery. At sites of close contact between the endothelium and smooth muscle, localized gap junction connexins (Cx), endoplasmic reticulum (ER) 1,4,5-triphosphate receptors (IP_3R), and intermediate conductance calcium-activated potassium channels (IK_{Ca}) occur in close proximity with TRPC3. The localization and differential distribution of these channels and receptors suggests that these myoendothelial microdomains enable transfer of a connexin (Cx)-dependent endothelial hyperpolarizing current (**1**) and/or localized K^+ activity (**2,3**); with the net effect being smooth muscle hyperpolarization and endothelium-dependent relaxation (modified from;[7,34] see also *Figures 1* and *S7*). TRPC3-dependent calcium influx may activate myoendothelial K_{Ca} directly (**i**), and/or refill the IP_3R-mediated ER store (**ii**). Inward rectifying potassium channels (K_{ir}) are exclusive to the endothelium[6,13,55] and are activated by potassium in a feedback with K_{Ca} and Na^+/K^+-ATPase activity. DAG, diacylglycerol; E_m, membrane potential; MEGJ, myoendothelial gap junction; PLCβ, phospholipase C-beta; VDCC, voltage-dependent calcium channel.

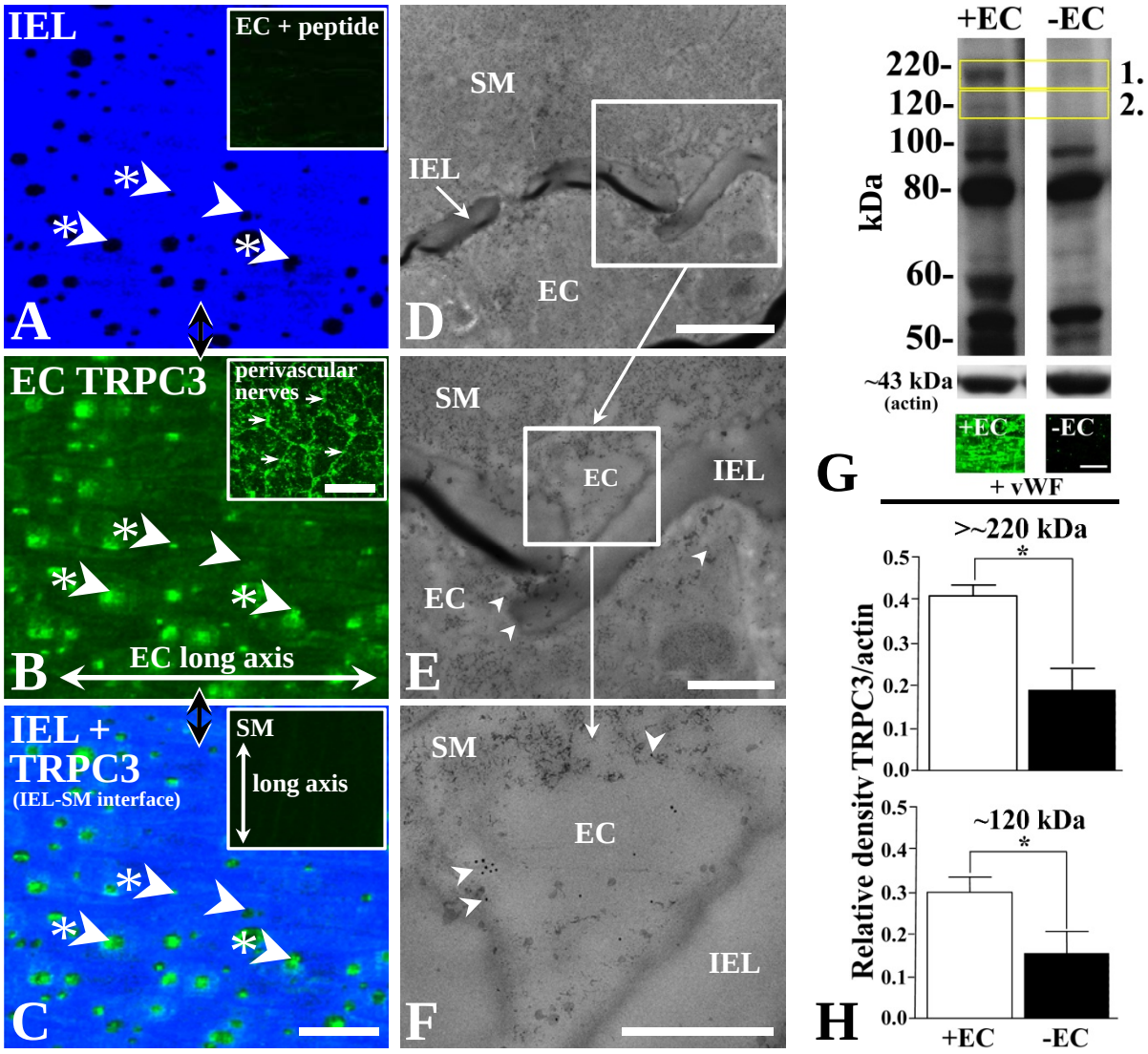

Figure 1.

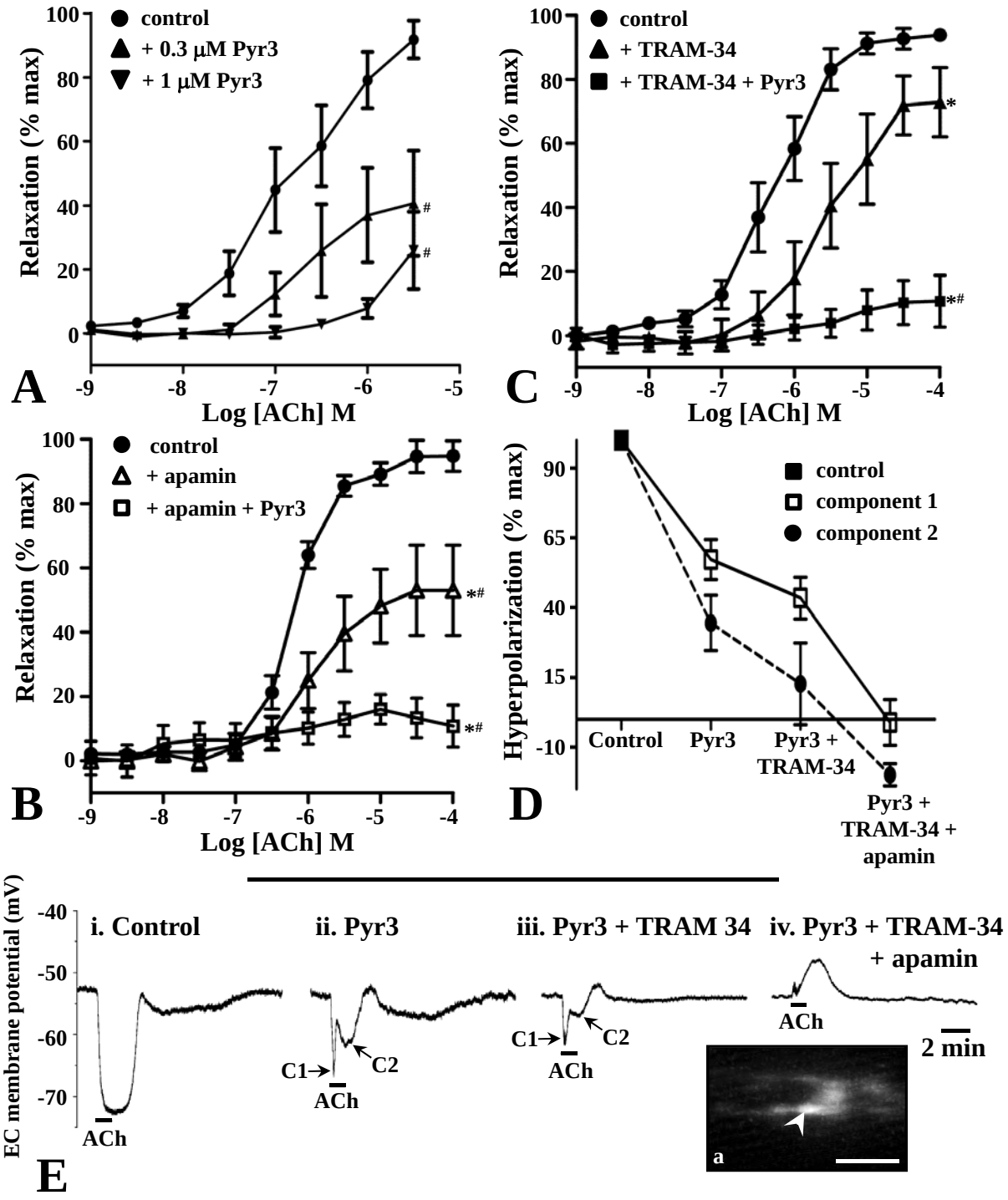

Figure 2.

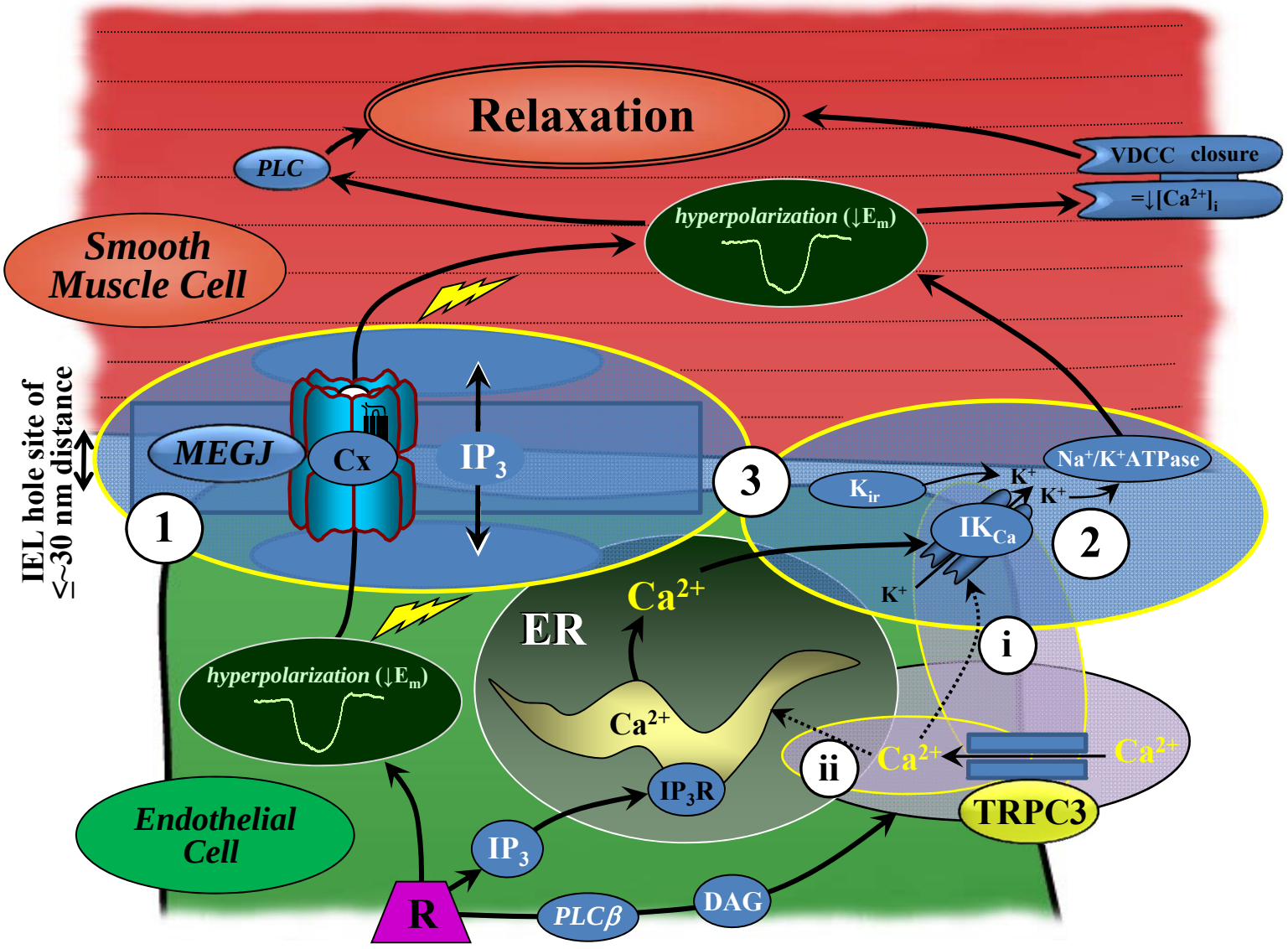

Figure 3.

Table 1 Internal elastic lamina (IEL) hole, TRPC3 and myoendothelial gap junction (MEGJ) characteristics (per 10^4 μm^2) in rat mesenteric artery.

IEL holes	IEL holes with TRPC3 plaques	IEL holes with no TRPC3	Number TRPC3 plaques	TRPC3 plaques not at IEL holes	MEGJ density
71 ± 7	52 ± 6	19 ± 6	60 ± 7	8 ± 2	16.3 ± 1.8

For IEL and TRPC3 characteristics, *n*=4, each from a different rat; each *n* being the mean data from four different randomly selected 10^4 μm^2 regions. For MEGJ characteristics, *n*=3 series of 5 μm of serial sections, each from a different animal. Data are mean ± SEM.

Table 2. Proportion of internal elastic lamina holes with localized channel densities in rat mesenteric artery.

TRPC3	IK_{Ca}*	$IP_3R^{\dagger}$	MEGJs (EM)	Cx37*	Cx40*
~73%	~80%	~75%	~23%	~28%	~31%

*from;[4] †from;[6] IK_{Ca}, intermediate conductance calcium-activated potassium channel; IP_3R, inositol 1,4,5-trisphosphate receptor. EM, from serial section electron microscopy analysis. See also Supplementary material online, *Figure S6.*

Table 3 Effect of drug interventions on endothelium-dependent vasodilation in rat mesenteric arteries.

	pEC_{50}	E_{max}	n
Vehicle	6.4 ± 0.1	94.3 ± 2.1	14
L-NAME (100 μM) + ODQ (10 μM) + indomethacin (10 μM)	6.9 ± 0.2	86.1 ± 5.0	10
L-NAME / ODQ + indomethacin + Pyr3 (0.3 μM)	6.8 ± 0.2	38.5 ± 16.6*,†	6
L-NAME / ODQ + indomethacin + Pyr3 (1 μM)	-	26.0 ± 12.1*,†	5
L-NAME / ODQ + indomethacin + TRAM-34 (1 μM)	5.4 ± 0.3*,†	72.9 ± 10.8	7
L-NAME / ODQ + indomethacin + TRAM-34 + Pyr3 (1 μM)	-	10.7 ± 8.1*,†,‡	7
L-NAME / ODQ + indomethacin + apamin (50 nM)	5.6 ± 0.2*,†	53.0 ± 11.8†	7
L-NAME / ODQ + indomethacin + apamin + TRAM-34	-	13.1 ± 5.6*	3
L-NAME / ODQ + indomethacin + apamin + Pyr3 (1 μM)	-	10.8 ± 5.5*,†,§	7
L-NAME / ODQ + indomethacin + apamin + TRAM-34 + Pyr3	-	1.3 ± 2.8*	4

Data are mean ± SEM.

$^{*}P<0.05$, significant compared to vehicle.

$^{\dagger}P<0.05$, significant compared to L-NAME + ODQ + indomethacin.

$^{\ddagger}P<0.05$, significant compared to L-NAME + ODQ + indomethacin + TRAM-34.

$^{\S}P<0.05$, significant compared to L-NAME + ODQ + indomethacin + apamin.

Transient receptor potential canonical type 3 channels facilitate endothelium-derived hyperpolarization-mediated resistance artery vasodilator activity

---

Supplementary Data

Supplementary Methods, Results, Discussion and Tables

2. Methods

2.1 Animals and tissue

Adult male Sprague Dawley rats were anaesthetised with sodium pentathol (100 mg/kg; ip), and ~300 μm diameter 1st-3rd order mesenteric arteries dissected in Krebs' solution containing (in mM): 112 NaCl, 25 $NaHCO_3$, 4.7 KCl, 1.2 $MgSO_4.7H_2O$, 0.7 KH_2PO_4, 10 HEPES, 11.6 glucose, 2.5 $CaCl_2.2H_2O$; pH 7.3. Male 8-10 week old TRPC3 KO mice[1] generated on a 129SvEv/C57BL/6J mixed background and age-matched littermate WT controls were anaesthetized with isofluorane and the aorta dissected in Hank's balanced salt solution for imaging studies. Rat liver, and mouse liver, aorta and mesenteric arteries were also dissected from anaesthetized (sodium pentathol; 100 mg/kg; ip) animals for reagent characterization studies. Respiration rate and tactile responses were monitored to indicate adequacy of anaesthesia.

KO and WT mice were genotyped via PCR amplification of the genomic TRPC3 DNA. The genotyping confirmed the omission of exon 7 of the TRPC3 gene in the KO mice as reported by Hartmann et al.[1]

All procedures conform with the Guide for the Care and Use of Laboratory Animals published by the US National Institutes of Health (NIH Publication No. 85-23, revised 1996),

and were approved by the Animal Experimental Ethics Committees of the University of New South Wales (09/43B) and Monash University (SOBSA/P/2007/100), and the Animal Protocol Review Committee, Baylor College of Medicine (AN-4366).

2.2 Reagent characterization

TRPC3 antibody specificity was determined by immunohistochemistry using stably transfected HEK-293 cells expressing mouse TRPC3 (Supplementary material online, *Figure S1A-C*), and by confocal immunohistochemistry (Supplementary material online, *Figures S1D-I, S2A*) and Western blotting using extracts of tissues from rat (Supplementary material online, *Figure S3*). Primary antibody and primer characteristics are detailed in Supplementary material online, *Tables S1* and *S2*.

The specificity of the putative TRPC3 blocker Pyr3 (ethyl-1-(4-(2,3,3-trichloroacrylamide)phenyl)-5-(trifluoromethyl)-1H-pyrazole-4-carboxylate)[2] was validated by pressure myography in mesenteric artery from KO and WT mice, patch clamp using freshly isolated mouse mesenteric artery endothelial cells (Supplementary material online, *Figure S5*) and transfected HEK cells expressing TRPC3 (Supplementary material online, *Figure S4*) and by calcium imaging using aortic endothelial cells obtained from KO and WT mice (Supplementary material online, *Figure S2B*).

2.3 Western blotting

The specificity of TRPC3 antibody and characteristics of TRPC3 channels in adult male Sprague Dawley rat mesenteric artery were determined using Western blotting. Rat mesenteric arteries and liver, and mouse liver were rapidly frozen, and stored in liquid nitrogen. Tissues were ground using a mortar and pestle, resuspended in phosphate buffered saline (PBS), pH 7.4, containing

protease inhibitor cocktail (Roche Diagnostics, Castle Hill, Australia) and centrifuged (3000 x g, 4ºC; 5 minutes). The supernatant was removed and placed on ice, and the pellet snap frozen and reprocessed as above. Supernatants were then pooled and centrifuged (20,000 x g, 4ºC; 1 hour). Supernatants containing 'soluble' protein (containing soluble cytosolic proteins and any residual fragments of unpelleted membranes) were separated, aliquoted, rapidly frozen in and stored in liquid nitrogen. Pellets with 'membrane-enriched' protein (containing plasma, endoplasmic reticulum, mitochondria, Golgi, lysosome and peroxisome membrane proteins) were suspended in PBS containing protease inhibitor cocktail (Roche Diagnostics, Castle Hill, Australia) with 0.1% Triton X-100. Samples were aliquoted, rapidly frozen in liquid nitrogen and stored at -80˚C. Protein concentration of the samples was determined using a Bradford protein assay kit (Bio-Rad, Australia).

Aliquoted protein extracts (5, 10 or 20 µg protein) were dissolved in lithium dodecyl sulfate (LDS) sample buffer (0.5% LDS, 62.5 mM Tris-HCl, 2.5% glycerol, 0.125 mM EDTA), pH 8.5, 10 minutes at 70ºC. The samples were separated by electrophoresis in 4-12% bis-Tris polyacrylamide gels (Invitrogen, Australia) using MOPS-SDS running buffer and electroblotted onto PVDF membranes overnight at 4˚C, according to manufacturer's recommendations (Invitrogen). Following protein transfer, blots were thoroughly washed, blocked and probed with TRPC3 antibody (batches AN-02, 03, 06 or 07; Supplementary material online, *Table S1*), and specific binding visualized using alkaline phosphatase-conjugated secondary antibody and chemiluminescence according to the manufacturer's instructions (Invitrogen). Band sizes were estimated by comparison of migration distance with Magic Mark XP protein standards (Invitrogen). The intensity of the bands corresponding to TRPC3 protein expression were determined using Photoshop CS3 (Adobe, CA, USA), normalised with corresponding actin bands and statistically analysed (GraphPad Prism, CA, USA).

To verify potential endothelial or smooth muscle cell TRPC3 expression, samples were prepared for Western blotting using rat mesenteric artery from which the endothelium had been disrupted. In freshly dissected intact vessel segments, successive and vigorous passing of a 50 μm diameter wire through the lumen disrupted the endothelium, with subsequent flushing of the lumen with Krebs solution via a micropipette to remove cellular debris. A small segment of endothelium-damaged artery was processed for confocal immunohistochemistry as described below, and compared with intact vessels for the presence of the specific endothelial marker, vWF, as confirmation of endothelial disruption.

To clarify specificity, TRPC3 antibody was incubated with its cognate peptide in order to block specific binding. Prior to use, peptide was added to antibody in a 1:10 ratio (v/v), mixed and incubated at 37˚C for 1 hour, then overnight at 4˚C. The blocked antibody was then used in Western blotting detection as above.

2.4 Cell culture

HEK-293 cells (Invitrogen), were cultured to 90% confluence in DMEM (Invitrogen, Australia) supplemented with 10% fetal bovine serum in a humidified atmosphere of 95% O_2/5% CO_2 at 37ºC. Cells were transfected with mouse TRPC3 cDNA cloned into a pIRES-DsRed2 vector construct (Clontech, CA, USA) using Lipofectamine, 2000 (Invitrogen, Australia), according to manufacturer's instructions. Cells were treated with 1100 μg/ml of G418 antibiotic (Invitrogen, Australia) for 4 weeks to select for stably transfected cells. The expression of mouse TRPC3 gene in the G418 resistant cells was verified by PCR amplification and sequencing of the TRPC3 cDNA transcript (primer characteristics; Supplementary material online, *Table S2*).

The sequencing of TRPC3 cDNA was made by PCR amplification of the cDNA using the BigDye Terminator V3.1 sequencing reaction mix according to the manufacturer's protocol

(Applied Biosystems, USA). The reaction product was then analyzed using ABI 3730 Capillary Sequencer (Applied Biosystems, USA) to obtain the sequence information. The TRPC3 cDNA sequence was verified via comparison with the mouse TRPC3 mRNA sequence in the NCBI database (accession no. NM_019510.2).

2.5 Mouse aortic endothelial cell calcium imaging

Aortic endothelial cells were obtained from mouse aorta explants grown on BD Matrigel™ Basement Membrane Matrix (BD Biosciences, CA, USA) as described by Suh *et al.*[3] Briefly, 35 mm culture dishes were coated with BD Matrigel, diluted 1:1 with DMEM containing glucose and L-glutamine (Gibco, CA, USA) for 1-2 hour at room temperature. The excised aorta was carefully cleaned of blood and extraneous tissue, washed in PBS, cut into 2 mm rings and transferred to Matrigel-coated dishes, containing DMEM supplemented with 10% FBS (Gibco), 100 μg/ml Endothelial Cell Growth Supplement (BD Biosciences), 10 U/ml heparin (Sigma, MO, USA), 100 U/ml penicillin/streptomycin (Invitrogen, CA, USA) and 2% Minimal Essential Amino Acid mixture (Sigma). Aortic rings were cut open, placed intima-down on the gel surface and allowed to grow for 4-12 weeks to allow endothelial cells to proliferate and spread throughout the Matrigel. For calcium imaging experiments, endothelial cells were harvested from Matrigel culture following 1 hour incubation with neutral protease (7 mg/ml) in PBS, after which the cells were washed twice with cell culture medium, resuspended and plated onto 12 mm glass coverslips coated with fibronectin (BD Biosciences) and used between day 3 and 10 after the passage.

At the time of experimentation, cells were loaded with Fura-2AM (TefLabs, TX, USA) for 1 hour at 1 μg/ml and imaged by acquiring 340/380 nm fluorescent ratios every 4 seconds, using an Olympus IX81 fluorescent microscope equipped with Uplan S-Apo 20x 0.75 NA lens

(Olympus, USA), Lambda LS Xenon Arc lamp, Lambda 10-2 filter wheel shutter controller (both from Sutter Instruments, CA, USA), RET-EXi-F-M-12-C CCD-camera (QImaging, Canada) and controlled with Slidebook 4.2 Imaging software (Olympus). Experiments were performed at room temperature and continuous bath perfusion using an RC-25 bath (Warner Instruments, CT, USA). Extracellular bath solution contained (in mM): 140 NaCl, 5.6 KCl, 1.6 $CaCl_2$, 1 $MgCl_2$, 10 glucose, 10 HEPES, pH 7.3. Endothelial calcium responses to the muscarinic agonist CCh (100 μM) were measured for vehicle control (0.1% DMSO) and in the presence of Pyr3[2] for WT and KO derived cells. DMSO or Pyr3 was administered 5 minutes prior to commencing the calcium recording. Background fluorescence was determined from a region without cells, and was subtracted prior to ratio determination.

2.6 Immunohistochemistry

2.6.1 Fluorescence microscopy. HEK-293 cells expressing TRPC3 were fixed in 4% paraformaldehyde in PBS for 10 minutes, washed with PBS and permeabilized with 1% Triton X-100 in PBS, followed by overnight incubation with TRPC3 antibody (batch AN-03; Supplementary material online, *Table S1*) in PBS with 2.5% normal goat serum (Vector Laboratories, CA, USA). After washing, cells were incubated with AlexaFluor 488 (1:500; Invitrogen, A11008) secondary antibody in PBS for 6 hours. Following washing in PBS, cells were visualized using a Leica DMIL inverted microscope with a 40 x HCX PL Fluotar (0.75 NA) objective and I3 filter block (Leica, Mt Waverly, Australia; Ex 450-490 nm dichroic 510 Em LP 515). Images were captured using an Andor emCCD IXon camera at 1 megapixel (MP). Peptide block involved pre-incubation of primary antibody in a 1:5 (v/v) excess of the immunizing peptide (Supplementary material online, *Table S1*).

2.6.2 Confocal microscopy. The distribution of TRPC3 was examined in rat mesenteric artery, and KO and WT mouse aorta and mesenteric artery, using conventional confocal immunohistochemistry as previously described.[4,5] The distribution of vWF was examined and arteries in which the endothelium had been disrupted compared to intact artery. Briefly, rats were perfused via the left ventricle with a clearance solution of 0.1% bovine serum albumin (BSA), 10 U/ml heparin and 0.1% $NaNO_3$ in saline, to fully dilate the vessels, and subsequently fixed with 2% paraformaldehyde in 0.1 mM PBS. To optimize the area visible in the narrow focal region of the IEL holes and associated potential channel localization at the IEL-smooth muscle or endothelial cell interface, as sites of potential myoendothelial microdomains,[4,5] tubular vessel segments were cut along the lateral plane and pinned out as a flat sheet with the intima uppermost.[4,6] In addition, some fresh vessel segments were opened, as above, and incubated for 10 minutes in Krebs' solution containing 0.1% $NaNO_3$, prior to fixation in 2% paraformaldehyde in PBS for 10 minutes, or acetone at 4^{o}C for 5 minutes. Whole mount tissues were then incubated in blocking buffer, as PBS containing 1% BSA, 0.2% Triton X-100, for 2 hours at room temperature, rinsed in PBS (3 × 5 minutes) and incubated in primary antibody to TRPC3 or vWF in blocking buffer for 18 hours at 4°C (antibody characteristics, Supplementary material online, *Table S1*). Tissue was then rinsed in PBS (3 × 5 minutes) and incubated in secondary antibody (AlexaFluor 633; Invitrogen, A21070 for rat, and A21050 for mouse) diluted in 0.01% Triton X-100, for 2 hours, and further rinsed in PBS (3 × 5 minutes), mounted intima uppermost in anti-fade glycerol and examined using matched settings on a confocal microscope (FV1000; Olympus, North Ryde, Australia). Cell integrity was verified in samples of tissue via propidium iodide (0.002% in mounting media) nuclear staining. In addition to clarifying TRPC3 antibody specificity using Western blotting, transfected cells and KO mouse tissue, mesenteric artery controls involved pre-incubation of primary antibody in a 1:5 (v/v) excess of the immunizing

peptide (Supplementary material online, *Table S1*), omission of the primary, and substitution of the primary for an unrelated IgG, using the confocal labeling protocol, as above; as well as using immunoelectron microscopy data. The IEL was visualized using autofluorescence at 488 nm.

For semi-quantitative estimation of endothelial TRPC3 expression, relative pixel fluorescence density was determined using CellR software (Olympus), and a smooth muscle signal of zero, since TRPC3 are absent in these cells of this vessel.[7] The mean fluorescence density of 10 randomly selected regions of interest, as apparent TRPC3 densities at IEL hole sites, and equivalent areas 5 μm adjacent to these areas, from each of 4 different preparations from a different animal, were determined. For comparative rat and KO mouse mesenteric artery smooth muscle fluorescence density measurements, 8 x 100 μm^2 selected regions of interest from 4 different preparations, each from a different animal, respectively, were examined.

2.6.3 Electron microscopy. Tissue preparation for immunoelectron microscopy was as previously described.[4,8] In brief, 1-2 mm long mesenteric artery segments were rapidly dissected from heavily anaesthetized animals and frozen at high pressure (Leica bulk high pressure freezer; ~2,100 bar), freeze-substituted (Leica AFS; -90°C) in 0.1% uranyl acetate in acetone over 4 days, infiltrated, and embedded in LR gold at -25°C, and polymerized under UV light. Individual serial thin transverse sections (~100 nm) were mounted on Formvar- and carbon-coated slot grids and processed for antigen localization as for confocal immunohistochemistry, although the secondary used was 10 nm colloidal gold-conjugated antibody (1:40; 2 hours) in 0.01% Tween-20. Controls included peptide block and omission of the primary antibody. Sections were stained conventionally with lead citrate, with tissue from 3 animals being examined.

Tissue preparation and analysis for conventional serial section electron microscopy, and serial section analysis for determining myoendothelial gap junction density, was as previously

described.[5] The IEL and the associated endothelial and smooth muscle cell regions were examined, and areas of labelling and myoendothelial gap junctions imaged at x10-40,000 on a Phillips 7100 transmission electron microscope at 16 MP (camera from Scientific Instruments and Applications, Duluth, USA).

2.7 TRPC3 and EDH-mediated vasodilation - pressure myography

The characteristics of TRPC3 channels in adult male Sprague Dawley rat mesenteric artery were determined using pressure myography. Freshly dissected rat (internal diameter in 0 mM calcium, 287 ± 6 μm; *n*=15) and mouse mesenteric arteries (internal diameter in 0 mM calcium, control, 175 ± 8 μm; *n*=4; TRPC3 KO, 167 ± 8 μm; *n*=6) were cannulated in a pressure myograph (Living Systems, Vermont, USA) and continuously superfused with Krebs' solution (37^{o}C) at a rate of 3 ml/minute. Arteries were pressurized to 80 mmHg with incremental increases over 80 minutes. Vessels were initially pre-constricted with superfused PE (1 μM; to 80% of maximum constriction), which was present in all experiments. Endothelium-dependent vasodilation in rat mesenteric arteries was evoked with increasing concentrations of ACh (1 nM-30 μM) added cumulatively to the bath; whilst the response in mouse mesenteric artery was evoked using the PAR-2 agonist, SLIGRL at 10 μM.[9]

Experiments were conducted in the presence of L-NAME (100 μM), ODQ (10 μM), and indomethacin (10 μM), as well as the putative TRPC3 blocker, Pyr3 (1 μM for 20 minutes[2]) apamin (15 minutes; 100 nM), and / or TRAM-34 (30 minutes; 1 μM), ; the latter two agents as defining blockers of EDH.[10-12], prior to addition of ACh or SLIGRL. Additional experiments on rat mesenteric artery were also performed in the absence of L-NAME, ODQ and indomethacin. Artery diameter changes are expressed as a percentage of the maximal dilation achieved by

replacing the control Krebs' solution with calcium-free Krebs' solution at the end of the experiment.

2.8 TRPC3 and EDH - sharp electrode electrophysiology

The characteristics of TRPC3 channels in adult male Sprague Dawley rat mesenteric artery were also determined using endothelial cell membrane potential recordings. Freshly dissected rat mesenteric arteries were cut along the longitudinal axis and pinned endothelium uppermost to the base of a recording chamber and continuously superfused as described previously.[5] L-NAME (200 μM) and indomethacin (1 μM) were present in all experiments. The membrane potential of endothelial cells was recorded using intracellular glass microelectrodes containing 1 M KCl (100-140 MΩ resistance and an Axoclamp 2B amplifier: Axon Instruments, USA) and the tips were filled with Lucifer Yellow CH to allow unequivocal identification of every impaled cell.[5] Endothelial cells were stimulated with 1 μM ACh for 1 minute. Responses were recorded in the absence (control) and presence of Pyr3 (1 μM), TRAM 34 (5 μM) and apamin (100 nM). Responses recorded in the presence of blockers were expressed as a percent of the control response in L-NAME and indomethacin.

2.9 TRPC3 currents - patch clamp electrophysiology

For voltage clamp recordings, HEK-293 cells stably expressing recombinant TRPC3 channels were grown to 85-95% confluence on a coverslip coated with poly-D-lysine and collagen (Type IV from human placenta). Prior to recording, the cells were incubated in the bath solution, as HEPES-buffered physiological salt solution, containing (in mM): NaCl, 120; KCl, 5.4; $MgCl_2$, 1.13; glucose, 10; HEPES, 20, pH 7.3 (adjusted with NaOH) for 10 minutes, with the treatment group containing Pyr3 in the bath solution. Recording pipettes were made from borosilicate glass

(GC120TF-10, Harvard Apparatus, UK). The pipette resistance was at 3-6 MΩ and filled with internal solution containing (in mM): CsCl, 130; $MgCl_2$, 2.0; EGTA, 10; ATP, 0.3; GTP, 0.03; pH at 7.3 (adjusted with CsOH). Whole cell patch clamp recordings were made using an Axopatch 200 or Multiclamp 700B patch clamp amplifiers (Molecular Devices, CA, USA) controlled by pClamp v.10.2 software (Molecular Devices). The membrane was clamped at a holding voltage of -40 mV, and a voltage ramp (-100 to +50 mV) over 1 second was applied every 5 seconds.

Freshly dispersed mesenteric endothelial cells used in electrophysiological experiments were obtained from $Cx40^{BAC}$-GCaMP2 mice[13] by enzymatic dissociation (70 minutes at 37^{o}C) using neutral protease (8 U/ml) and elastase (2 U/ml) mg/ml in the following digestion buffer (in mM): 138 NaCl, 5 KCl, 1.5 $MgCl_2$, 0.42 Na_2HPO_4, 0.44 NaH_2PO_4, 0.1 $CaCl_2$, 10 HEPES, 4.2 $NaHCO_3$ and 0.3% BSA. These cells were used as when isolated they are easily identifiable via fluorescence microscopy. This was followed by a 1 minute incubation with collagenase type 1 (120 U/ml) in the same digestion buffer. All enzymes were obtained from Worthington (Lakewood, NJ, USA). Dispersed endothelial cells were placed in the recording chamber and identified by green fluorescence (GFP emission filter) using same microscope set up as described under Ca^{2+} imaging section. Whole cell currents of EC were recorded in the voltage clamp mode using the perforated patch configuration.[14] The series resistance was maintained at or below 20 MOhm and was not compensated. The pipette solution contained (in mM) 40 KCl, 100 K gluconate, 1 $MgCl_2$, 10 NaCl, 0.1 EGTA, 10 NaCl, 10 HEPES, 0.1 EGTA (pH 7.2, adjusted with KOH). Extracellular bath solution (in mM): 140 NaCl, 5.6 KCl, 1.6 $CaCl_2$, 1 $MgCl_2$, 10 glucose, 10 HEPES, pH 7.3. Endothelial cells were held at -70 mV and whole cell currents were evoked by 1 second voltage ramps from -120 to +60 mV every 3 seconds. All experiments were done at

room temperature. Of note, potassium currents activated by ATP or NS 309 were analyzed after subtraction of baseline current, recorded before the agonist application.

2.10 Statistics

Agonist concentrations causing half-maximal responses (EC_{50} value) were calculated using non-linear regression analysis (GraphPad Prism) and expressed as the negative logarithm of the molar concentration (pEC_{50} values). Percentage vasodilation evoked by [agonist] was taken as the maximum (peak) responses (E_{max}). All data are expressed as mean ± SEM from '*n*' experiments each from a different animal, and were determined by one-way analysis of variance followed by Dunnett's post-test for multiple comparisons, or paired *t* tests for groups of two. Calcium imaging recordings from individual cells were averaged for each coverslip (12-59 cells/coverslip). The number of coverslips for each group was from 5 to 18 from a total of 3 WT and 3 TRPC3 KO mice. The average calcium responses per coverslip were then evaluated by two-way RM-ANOVA using the Holm-Sidak test for pair-wise multiple comparison procedures. A $P<0.05$ was considered significant.

2.11 Drugs and reagents

Electron microscopy reagents were from ProSciTech (Thuringowa, Australia), and unless otherwise stated, all other chemicals and drugs were from Sigma (Castle Hill, Australia or Saint Louis, USA), including Pyr3, or Tocris (Bristol, UK). Antibody source and characteristics are detailed in Supplementary material online, *Table S1*.

3. Results and Discussion

3.1 Rat mesenteric artery TRPC3

3.1.1 Protein localization

As a control for adequate rinsing steps in the confocal microscopy protocol, IgG alone was substituted for the primary at a matching concentration to the TRPC3 antibody in the primary antibody incubation step. Of note, when IgG alone (Supplementary material online, *Table S1*) was substituted for primary antibody, and the post-primary confocal protocol rinsing steps omitted, localized high level fluorescence densities at all internal elastic lamina (IEL) holes were present in rat mesenteric artery (data not shown); suggesting that IEL holes have an affinity for IgG; and emphasizing the importance of conducting adequate rinsing steps and control peptide block in the confocal immunohistochemistry protocol when examining whole mount vessel preparations.

3.2 Reagent characterization

3.2.1 TRPC3 antibody characterization

Specificity of the commercial Alomone TRPC3 antibody (ACC-016; Supplementary material online, *Table S1*) was demonstrated by immunohistochemistry using HEK cells expressing TRPC3 (Supplementary material online, *Figure S1A-C*) and segments of mesenteric arteries and aorta from TRPC3 KO and WT mouse (Supplementary material online, *Figures S1*, *S2A*, respectively), and also by Western blotting using tissue extracts of rat and mouse liver (Supplementary material online, *Figure S3*), and including primary antibody peptide block.

Four different batches of TRPC3 antibody were examined, with batches AN-02, 03 and 07 displaying consistent characteristics, whilst AN-06 did not, and was not used in subsequent work (Supplementary material online, *Table S1*). In fresh rat liver tissue extracts, TRPC3 antibody (batch AN-02) recognized an apparent monoglycosylated band at ~120 kDa, which is similar to published data for TRPC3 protein expressed in rat tissues,[15] as well as a likely TRPC3 complex

at >~220 kDa[16] and a likely breakdown product at ~60 kDa (Supplementary material online, *Figure S3*). Degradation products of TRPC3 in tissue extracts have been noted by Clarson *et al*.[15] Peptide block of the primary antibody abolished the staining of these bands (Supplementary material online, *Figure S3*) and non-specific bands remained unaffected. TRPC3 antibody batches AN-03 and AN-07 showed the same Western blot characteristics as AN-02, recognizing the same bands in the same fresh rat liver extracts (data not shown).

In rat mesenteric artery extracts, TRPC3 antibody recognized the same TRPC3 bands that were present in rat liver extracts, and also bands at ~110, 80, 40 and 20 kDa (Supplementary material online, *Figure S3*), which were abolished by peptide block and which we believe represent tissue-related differences in TRPC3 breakdown products. Every care was taken to minimize protein degradation during the removal and storage of tissues. However, in some time consuming procedures, such as the dissection of fine vessels and removal of extraneous tissues, some degradation is inevitable and has affected the strength of the remaining un-degraded TRPC3 signal, particularly in the case of the vascular endothelium which forms a small relative proportional mass of the total vessel wall.

3.2.1 Pyr3 / TRPC3 blocker characterization

3.2.1.1 Pressure myography

In pressurized WT and TRPC3 KO mouse mesenteric arteries, in the presence of L-NAME, ODQ and indomethacin, SLIGRL (PAR-2 agonist; 10 μM)-induced vasodilation was significantly attenuated in WT, but not KO in the presence of Pyr3 (1 μM; WT, 72 ± 7% SLIGRL control, 46 ± 9% with Pyr3, n=4, P<0.05; KO 75 ± 3% SLIGRL control, 64 ± 7 with Pyr3, n=6, P>0.05).

3.2.1.2 Calcium dynamics in cultured murine aortic endothelial cells

Carbachol (CCh; 100 μM) elicited a prolonged increase in $[Ca^{2+}]_i$ in WT and KO mouse aorta-derived primary culture endothelial cells (Supplementary material online, *Figure S2B*), and this calcium response was significantly attenuated by Pyr3 (10 μM) in WT-derived cells, over KO-derived cells (area under the curve; reduced by ~54% in WT, and by ~24% in KO). The inhibition of the early portion of the response in KO EC corresponds to the initial phase of internal store release. This initial phase comprises the first ~60 seconds of the response. The sustained component of the response (following the first 60 seconds) corresponds to the Ca^{2+} influx phase and was quite different between groups. Evaluation of individual time points by the Holm-Sidak test during the sustained phase demonstrated a significant difference for the time period out to 219 seconds of the WT response. However, the corresponding sustained phase in the KO EC was largely unaffected by Pyr3. For comparison, at the 150 second time point, there was a ~53% inhibition in the WT cells compared with only ~4% in the KO. Thus, it appears that Pyr3 is selective for TRPC3-mediated Ca^{2+} influx.

3.2.1.3 Whole cell patch clamp of transfected HEK-293 cells

Carbachol (100 μM) initiated a significant inward current (maximum, 266 ± 27 pA, *n*=6; Supplementary material online, *Figure S4A*) in transfected HEK cells expressing TRPC3 and clamped at -40 mV. This response was attenuated by ~84% and ~95%, in the presence of 2 and 10 μM Pyr3, respectively (to 37 ± 10 and 13 ± 9 pA, *n*=6 and 4, respectively; Supplementary material online, *Figure S4B, C*).

3.2.1.4 Whole cell patch clamp of mouse mesenteric artery endothelial cells

ATP (100 μM) evoked an outward K^+ current (at 40 mV) consisting of an initial peak followed by a more sustained component (Supplementary material online, *Figure S5A, B*). Pyr3 (3 μM) inhibited the ATP-induced K^+ currents in endothelial cells such that only an initial transient component remained (Supplementary material online, *Figure S5C, D*). Pyr3 was without effect on the maximal increases in K^+ current density evoked by the S/IK_{Ca} agonist NS309 (Supplementary material online, *Figure S5E, F*).

References

1. Hartmann J, Dragicevic E, Adelsberger H, Henning HA, Sumser M, Abramowitz J *et al.* TRPC3 channels are required for synaptic transmission and motor coordination. *Neuron* 2008;**59**:392-398.
2. Kiyonaka S, Kato K, Nishida M, Mio K, Numaga T, Sawaguchi Y *et al.* Selective and direct inhibition of TRPC3 channels underlies biological activities of a pyrazole compound. *Proc Natl Acad Sci USA* 2009;**106**:5400-5405.
3. Suh SH, Vennekens R, Manolopoulos VG, Freichel M, Schweig U, Prenen J *et al.* Characterisation of explanted endothelial cells from mouse aorta: electrophysiology and Ca^{2+} signalling. *Pflugers Arch* 1999;**438**:612-620.
4. Sandow SL, Neylon CB, Chen MX, Garland CJ. Spatial separation of endothelial small- and intermediate-conductance calcium-activated potassium channels (K_{Ca}) and connexins: possible relationship to vasodilator function? *Journal of Anatomy* 2006;**209**:689-698.
5. Sandow SL, Tare M, Coleman HA, Hill CE, Parkington HC. Involvement of myoendothelial gap junctions in the actions of endothelium-derived hyperpolarizing factor. *Circ Res* 2002;**90**:1108-1113.

6. Sandow SL, Haddock RE, Hill CE, Chadha PE, Kerr PM, Welsh DG *et al.* What's where and why at a vascular myoendothelial microdomain signaling complex? *Clin Exp Pharmacol Physiol* 2009;**36**:67-76.

7. Hill AJ, Hinton JM, Cheng H, Gao Z, Bates DO, Hancox JC *et al.* A TRPC-like non-selective cation current activated by alpha 1-adrenoceptors in rat mesenteric artery smooth muscle cells. *Cell Calcium* 2006;**40**:29-40.

8. Haddock RE, Grayson TH, Brackenbury TD, Meaney KR, Neylon CB, Sandow SL *et al.* Endothelial coordination of cerebral vasomotion via myoendothelial gap junctions containing connexins37 and 40. *Am J Physiol* 2006;**291**:H2047-H2056.

9. Beleznai T, Takano H, Hamill C, Yarova P, Douglas G, Channon K *et al.* Enhanced K^+-channel-mediated endothelium-dependent local and conducted dilation of small mesenteric arteries from ApoE-/- mice. *Cardiovasc Res* 2011;**92**:199-208.

10. McGuire JJ, Ding H, Triggle CR. Endothelium-derived relaxing factors: a focus on endothelium-derived hyperpolarizing factor(s). *Can J Physiol Pharmacol* 2001;**79**:443-470.

11. Sandow SL, Tare M. C-type natriuretic peptide: a new endothelium-derived hyperpolarizing factor? *Trends Pharmacol Sci* 2007;**28**:61-67.

12. Busse R, Edwards G, Feletou M, Fleming I, Vanhoutte PM, Weston AH. EDHF: bringing the concepts together. *Trends Pharmacol Sci* 2002;**23**:374-380.

13. Tallini YN, Brekke JF, Shui B, Doran R, Hwang SM, Nakai J *et al.* Propagated endothelial Ca^{2+} waves and arteriolar dilation in vivo: measurements in Cx40BAC-GCaMP2 transgenic mice. *Circ Res* 2007;**101**:1300-1309.

14. Rae J, Cooper K, Gates P, Watsky M. Low access resistance perforated patch recordings using amphotericin B. *J Neurosci Methods* 1991;**37**:15-26.

15. Clarson LH, Roberts VH, Hamark B, Elliott AC, Powell T. Store-operated Ca^{2+} entry in first trimester and term human placenta. *J Physiol* 2003;**550**:515-528.

16. Goel M, Sinkins WG, Schilling WP. Selective association of TRPC channel subunits in rat brain synaptosomes. *J Biol Chem* 2002;**277**:48303-48310.

17. Birnbaumer L, Zhu X, Jiang M, Boulay G, Peyton M, Vannier B *et al.* On the molecular basis and regulation of cellular capacitative calcium entry: roles for TRP proteins. *Proc Natl Acad Sci USA* 1996;**93**:15195-15202.

18. Vannier B, Zhu X, Brown D, Birnbaumer L. The membrane topology of human transient receptor potential 3 as inferred from glycosylation-scanning mutagenesis and epitope immunocytochemistry. *J Biol Chem* 1998;**273**:8675-8679.

19. Wu LJ, Sweet TB, Clapham DE. International union of basic and clinical pharmacology. LXXVI. Current progress in the mammalian TRP ion channel family. *Pharmacol Rev* 2010;**62**:381-404.

20. Zhu X, Jiang M, Peyton M, Boulay G, Hurst R, Stefani E, Birnbaumer L. TRP, a novel mammalian gene family essential for agonist-activated capacitative Ca^{2+} entry. *Cell* 1996;**85**:661-71.

21. Neylon CB, Nurgali K, Humme B, Robbins HL, Moore S, Chen MX, Furness JB. Intermediate-conductance calcium-activated potassium channels in enteric neurones of the mouse: pharmacological, molecular and immunochemical evidence for their role in mediating the slow afterhyperpolarization. *J Neurochem* 2004;**90**:1414-42.

22. Chadha PS, Haddock RE, Howitt L, Morris MJ, Murphy TV, Grayson TH *et al.* Obesity upregulates IK_{Ca} and myoendothelial gap junctions to maintain endothelial vasodilator function. *J Pharmacol Exp Ther* 2010;**335**:284-293.

23. Sandow SL, Senadheera S, Bertrand PP, Murphy TV, Tare M. Myoendothelial contacts, gap junctions and microdomains: anatomical links to function? *Microcirculation* 2012;**19**:DOI10.1111/j.1549-8719.2011.00146.x.

24. Dora KA, Gallagher NT, McNeish A, Garland CJ. Modulation of endothelial cell $K_{Ca}3.1$ channels during endothelium-derived hyperpolarizing factor signaling in mesenteric resistance arteries. *Circ Res* 2008;**102**:1247-55.

Table S1. Primary antibody characteristics.

Antibody (anti)	Raised against species / antigen	Antigen peptide block	Working dlution	Supplier, catalog and batch / lot number/s	Host
TRPC3*	Mse C' aa 822-835	yes	8 μg/ml, IHC / IEM 0.8 μg/ml HEK cell IHC 0.8 μg/ml Westerns	Alomone, ACC-016; batches AN-02,03,06[#],07	rabbit
vWF	Purified Hu vWF	no	1:300	Sigma, F3520	rabbit
IgG	Purified Rb IgG	no	5 μg/ml	Chemicon, PP64	rabbit

aa, amino acid; Hu, human; IEM, immunoelectron microscopy; IHC, immunohistochemistry; Mse, mouse; Rb, rabbit. *shares ~93% (13/14 residues) sequence identity with rat TRPC3. [#]AN-06 showed variability in Western blot and immunohistochemical characteristics compared to other TRPC3 antibody batches, and was thus not used in the primary aspects of this study.

Table S2. TRPC3 primer characteristics.

	Sequence (5' to 3')	Relative position from the start codon
Forward	CTAACTTTTCCAAATGCAGGAGGAGAAG	2135
Reverse	TCGCATGATAAAGGTAGGGAACACTAGA	2630

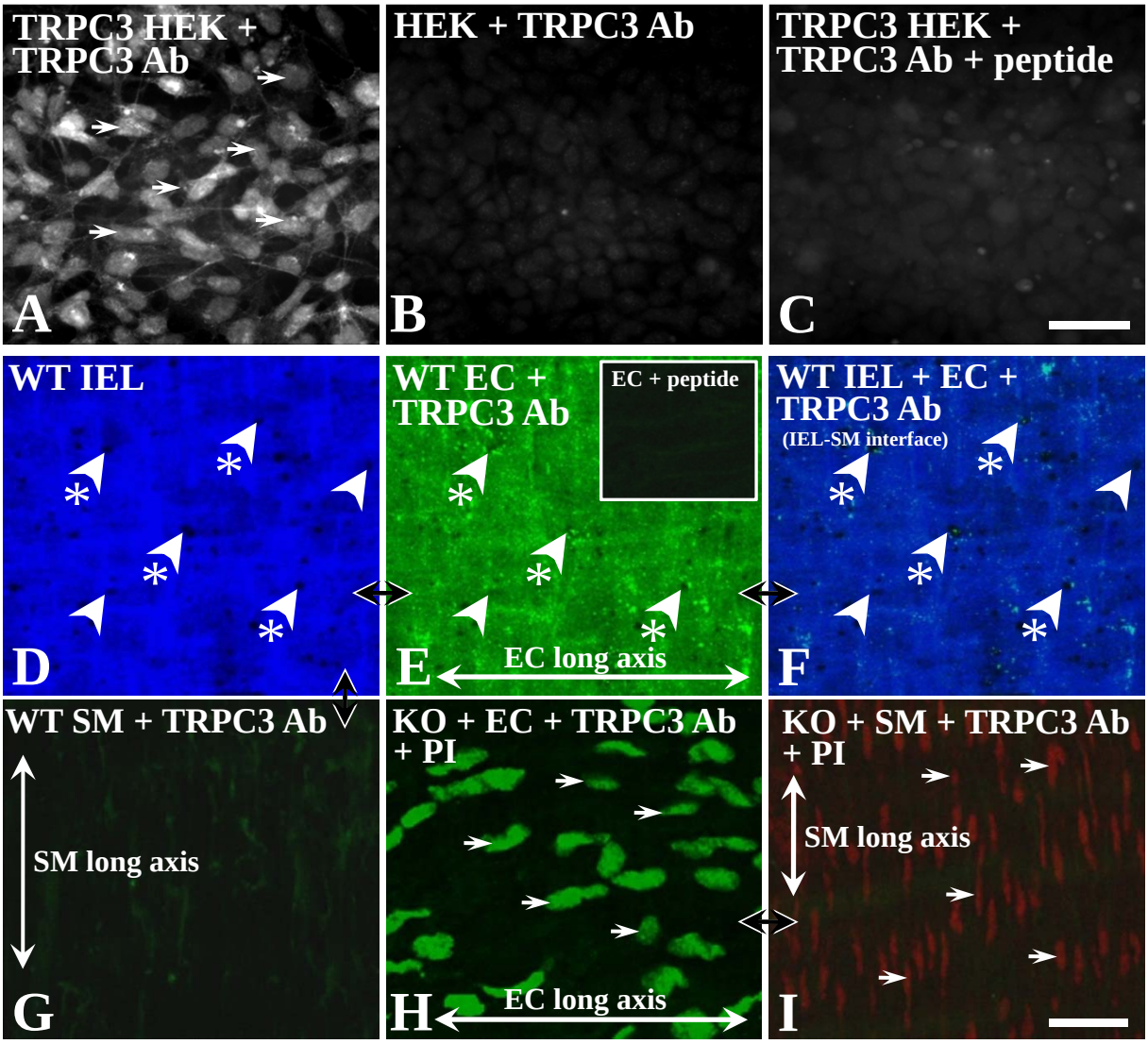

Figure S1. TRPC3 antibody characterization in transfected HEK cells and control and TRPC3 knock-out mouse mesenteric artery using immunohistochemistry. TRPC3 antibody (Ab; Alomone ACC-016; AN-03, shown as example; Supplementary material online, *Table S1*) specificity was supported via use of transfected cells expressing mouse TRPC3 cDNA. TRPC3 transfected HEK cells labelled with TRPC3 antibody (*A;* examples with arrows), whilst incubation of untransfected cells (*B*) and peptide block (*C*) show an absence of labelling, as did primary antibody omission, under the same conditions as *A* (data not shown). Consistent labelling was found using TRPC3 Ab batches AN-02, 03 and 07, whilst 06 showed an absence of labeling, and was not used in subsequent protocols. In mesenteric artery from control wild-type (WT) and TRPC3 knock-out (KO) mice (*D-G* and *H, I,* respectively), TRPC3 antibody (AN-07; Supplementary material online, *Table S1*) specificity was further characterized. TRPC3 confocal immunohistochemistry demonstrated the presence of TRPC3 in endothelial cells (EC), but not the smooth muscle (SM) of WT mesenteric artery (*E, F*, respectively). Similar to rat mesenteric artery (*Figure 1*), discrete holes are present in the internal elastic lamina (IEL) between the endothelium and smooth muscle (dark spots; *D, F*). Low level diffuse TRPC3 is localized to the endothelial membrane (*E*), whilst overlay of IEL and TRPC3 label at the IEL-SM focal plane border shows strong TRPC3 expression at a proportion of IEL holes (*F*; examples, arrowed with asterisks), as potential myoendothelial microdomain sites; noting that not all such sites have localized TRPC3 densities (examples with arrows, *D, F*). TRPC3 was absent in both cell layers of vessels from TRPC3 KO mouse (*H, I*). Peptide block abolished staining in WT mesenteric artery (*E*, inset), whilst cell layer patency was verified with propidium iodide (PI) nuclear staining (arrows, *H, I*, for example). The same vessel region is shown for WT and KO panels (*D-G* and *H, I,* respectively); with longitudinal vessel axis left to right. Internal elastic lamina (IEL) autofluorescence assisted with differentiation of cell layers (eg. *D*). *n*=3-4, each from a different animal. NB. *H, I* panels have been contrast/brightness enhanced in Photoshop. Scale bar, 50 μm (*A-C*), 25 μm (*D-I*).

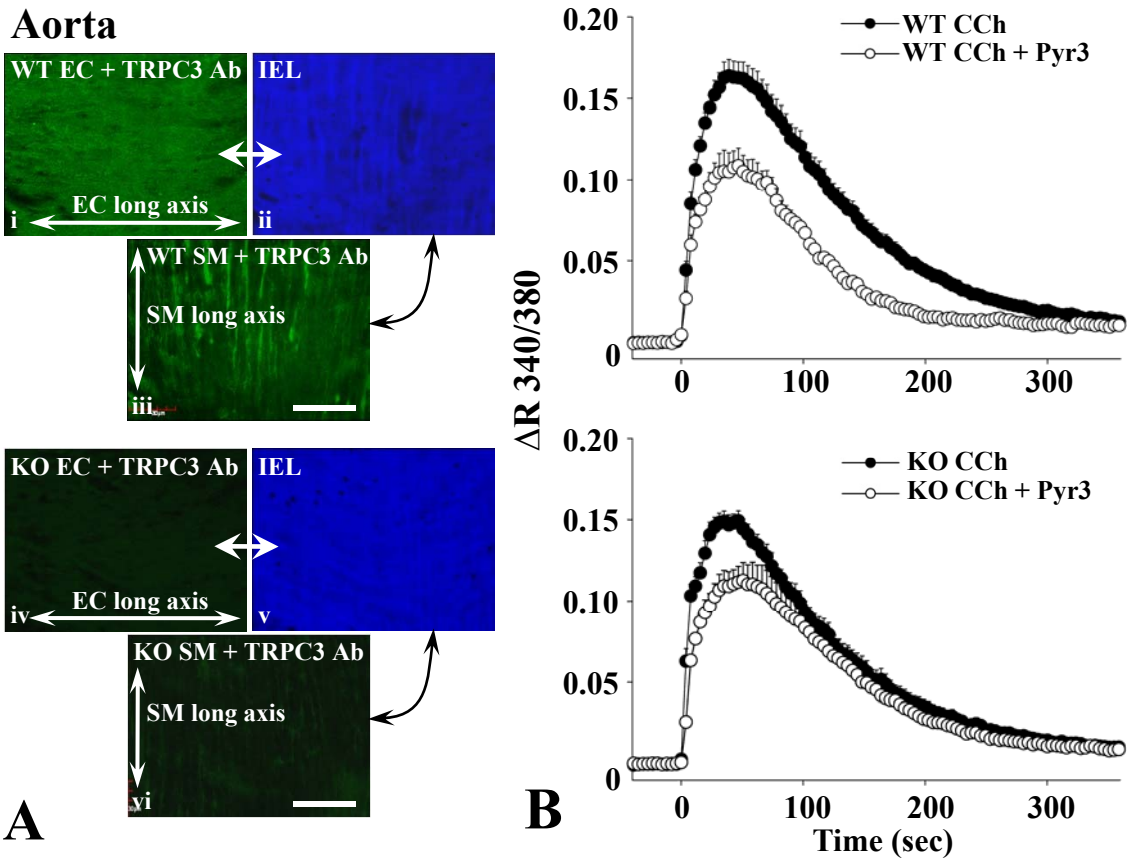

Figure S2. Mouse aorta TRPC3 distribution and agonist-induced calcium effects of Pyr3-block in isolated aortic endothelium. Antibody (Ab) specificity was further tested using TRPC3 knock-out (KO) and control wild-type (WT) tissue (*A*, *B*), with mouse genotypes being confirmed by PCR amplification of genomic DNA. TRPC3 antibody (AN-07; Supplementary material online, *Table S1*) confocal immunohistochemistry demonstrated the presence of TRPC3 in aortic endothelium (EC) and smooth muscle (SM; *A*). TRPC3 was absent in both cell layers of vessels from TRPC3 KO mouse (*A,iv,vi*). Peptide block abolished staining in WT aorta, whilst cell layer patency was verified with propidium iodide (PI) nuclear staining (see Supplementary material online, *Figure S2*, for example). The same vessel region is shown for WT and KO panels (*Ai-iii* and *iv-vi*, respectively); with longitudinal vessel axis left to right. Internal elastic lamina (IEL) staining assisted with differentiation of cell layers (*A,ii,v*). *n*=3-4, each from a different animal. Scale bar, 40 μm. TRPC3 blocker efficacy was tested using primary cultured aortic ECs derived from TRPC3 KO and WT mice. The putative TRPC3 blocker Pyr3 caused significantly larger attenuation of the sustained carbachol (CCh; 100 μM)-induced calcium response in control WT (*B*, upper), compared to TRPC3 KO (*B*, lower) ECs. Cells were preincubated with Pyr3 (10 μM) or 0.1% DMSO (control) for 5 minutes before recording. Calcium data represent the mean responses per coverslip ± SEM, obtained from three WT and three TRPC3 KO mice (*n*=3 different animals each, for WT and KO). The number of coverslips per group (*n*) were control WT, 18; WT + Pyr3, 5; KO control, 10; and KO + Pyr3, 5.

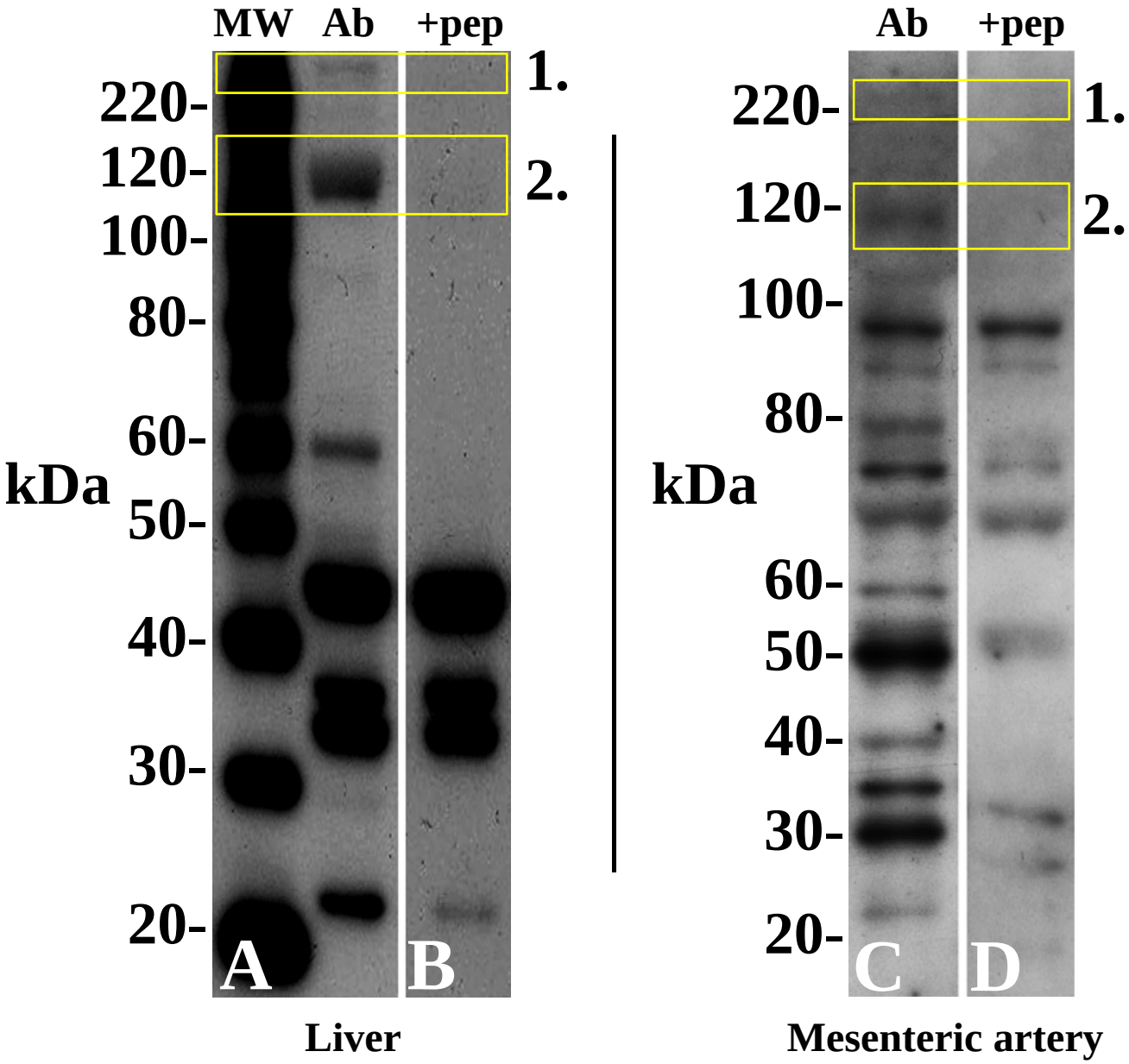

Figure S3. Western blot of TRPC3 protein expression in rat liver and mesenteric artery, with peptide block. Antibody (Ab) specificity was examined using control rat liver (*A, B*) and mesenteric artery (*C, D*) with peptide block. TRPC3 antibody batches AN-02 (as example used here), 03 and 07 (Supplementary material online, *Table S1*) were characterized using Western blotting. AN-02, 03 and 07 recognize monoglycosylated TRPC3 protein as a band at ~120 kDa (*A2*, boxed), whilst the band at >~220 kDa (*A1*, boxed) is probably an aggregate / undissociated TRPC3 channel complex, as a slow migrating band; whilst the ~60 kDa band is a likely breakdown product of the TRPC3 protein. Peptide block (+ pep) removed the TRPC3 bands (*B, D,* boxed, 1, 2). For liver, four lanes in total were run (two representative shown), with tissues from one rat per lane and loading of 5 μg of protein; whilst for the mesenteric artery three lanes in total were run with tissue from four different rats pooled together with loading of 10 μg of protein per lane. Incubation with a 1:10 (v/v), excess of peptide removed the TRPC3 bands (*B, D*, boxed, 1, 2). MW, molecular weight.

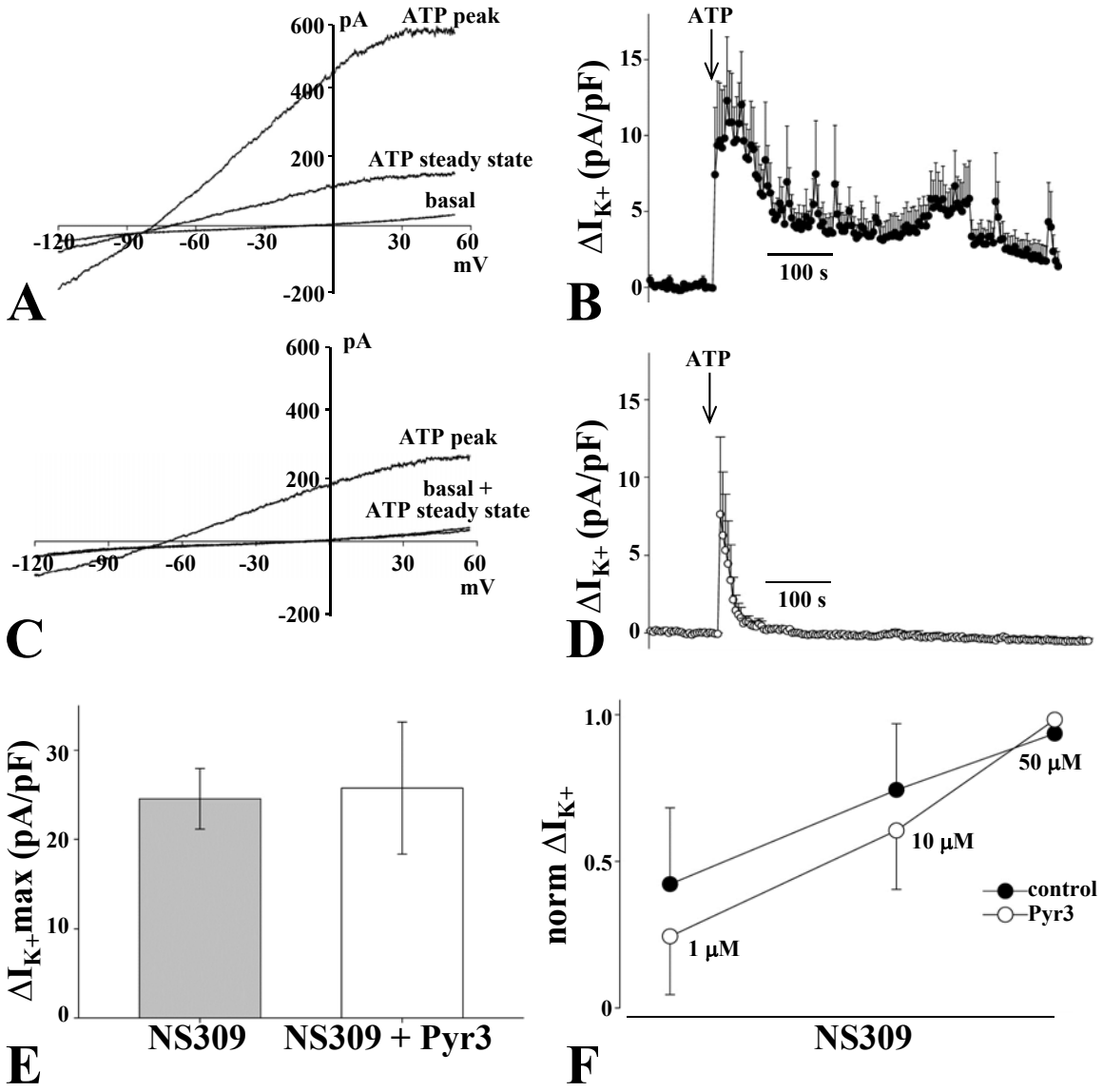

Figure S4. Pyr3 effect on agonist-induced K^+ currents in mouse mesenteric artery endothelial cells using patch clamp. ATP activates IK_{Ca}/SK_{Ca}-like potassium current in mesenteric artery endothelial cells (*A, B*). Representative I-V traces (*A*), and time-dependent changes in ATP (100 μM)-activated potassium current density; *n*=8 cells, from five mice (*B*). TRPC3 channel blocker Pyr3 (3 μM) inhibits ATP-activated potassium current (*C, D*; same protocol as *A, B*, respectively, but with addition of Pyr3). Representative I-V traces (*B*), and time-dependent changes in ATP-activated potassium current density in cells pretreated with Pyr3 (2-5 minutes before the ATP; *n*=4 cells, from four mice; *D*). Pyr3 (added 2-5 minutes before the NS309; *n*=5), had no effect on maximal potassium current density induced by the S/IK_{Ca} agonist NS309 alone (50 μM; *n*=4; *E*). Concentration-response plot (normalized to maximum) for potassium current density from a subset of cells exposed to NS309, with or without Pyr3 pretreatment (*n*=3 in each group; *F*). *B, D* were recorded at +40 mV. Mean ± SEM.

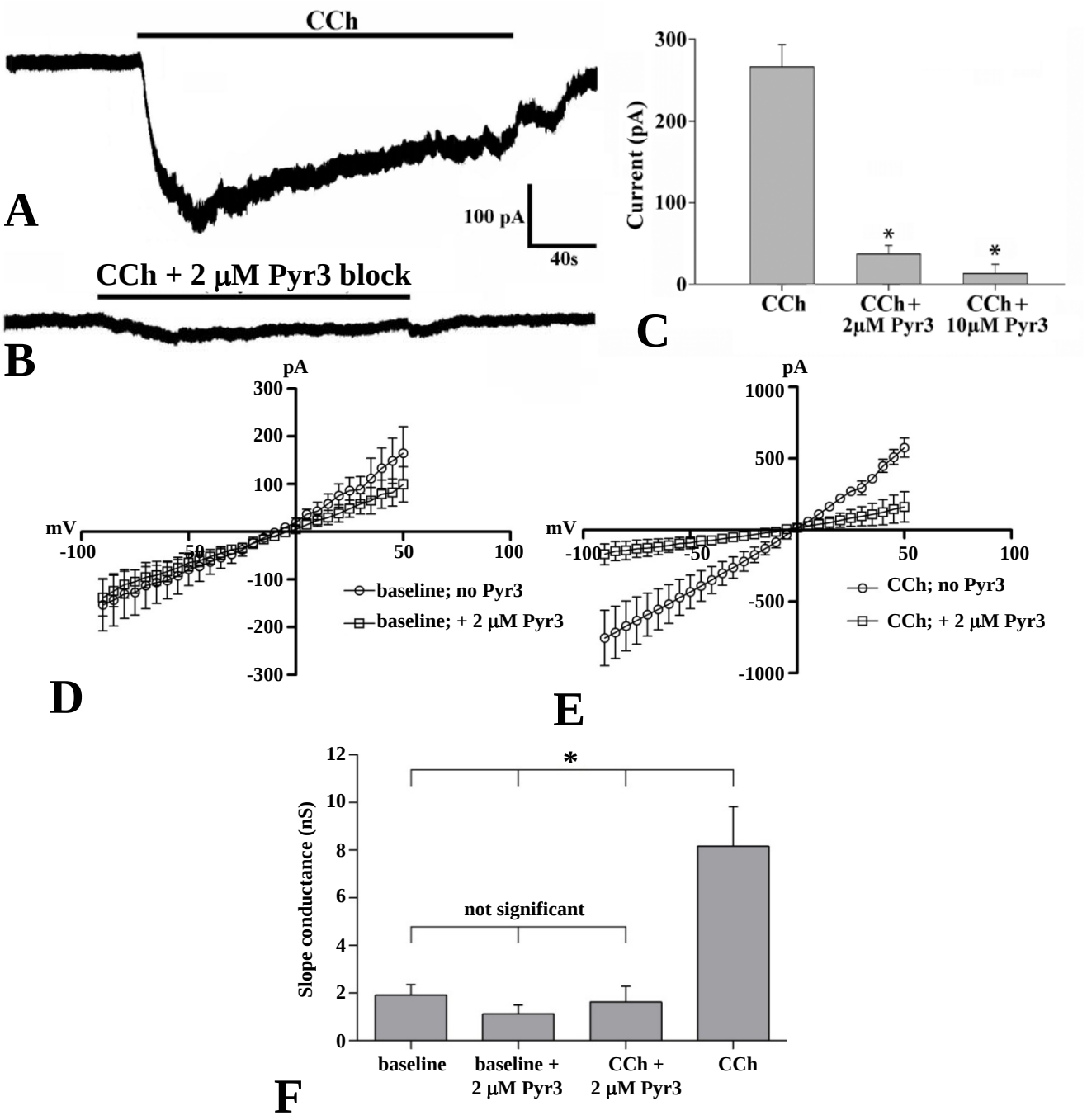

Figure S5. Characterization of specificity of Pyr3 block of TRPC3 channel conductance in HEK-293 cells.

The potency of the putative TRPC3 channel blocker Pyr3 was tested using patch clamped HEK cells transfected with TRPC3 plasmid. Carbachol (CCh; 100 μM)-activated an inward TRPC3 current (example, *A*) that was significantly attenuated by Pyr3 at 2 and 10 μM (*B*, *C*; *n*=6 and 4, respectively, vs *n*=6 for control CCh response). Current / voltage (I/V) relationships of baseline currents (*D*) show that Pyr3 has no significant effect on the intrinsic I/V profile; whilst I/V plots show Pyr3 block of CCh-activated inward and outward TRPC3 current (*E*). I/V plots were derived from voltage ramps over 1 sec; with data from an average of 3 cells per trace. Histogram of slope conductances (*F*, measured between -60 and -20 mV) for HEK293 cells expressing TRPC3 shows Pyr3 inhibition that returns CCh-activated TRPC3 conductance to baseline (*F*; *n*=5, for each group). Mean ± SEM. **P*<0.05, significant.

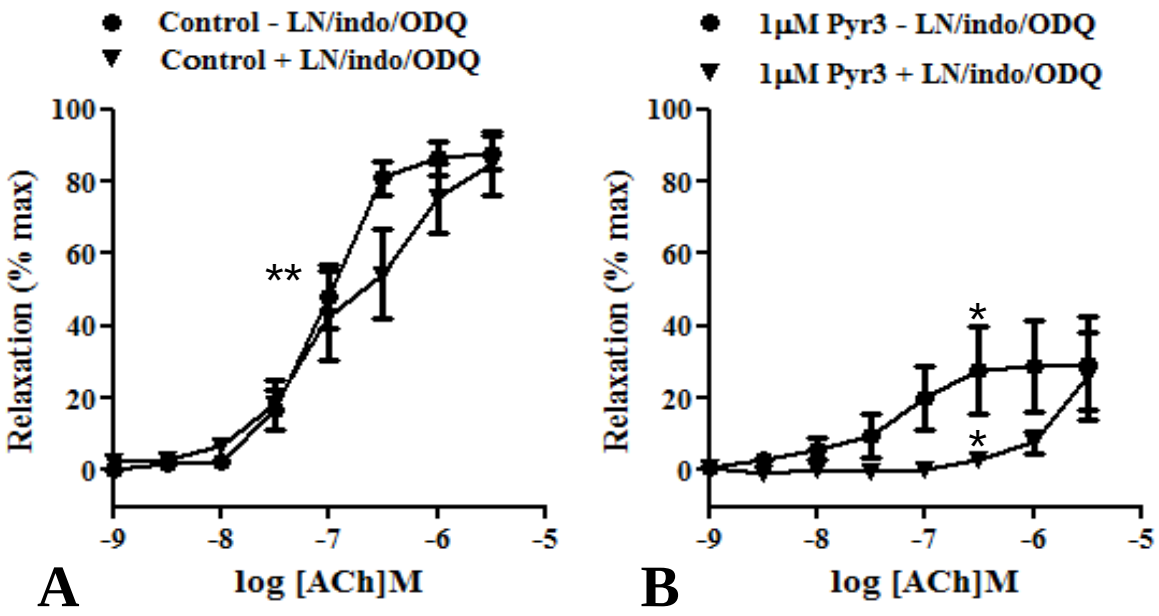

C	pEC_{50}	E_{max}	*n*
1. Vehicle (ACh)	**7.0 ± 0.1****	**87.9 ± 2.8**	**7**
2. Vehicle + L-NAME / ODQ, indomethacin	**6.4 ± 0.1****	**94.3 ± 2.1**	**14**
3. Vehicle + Pyr3 (1 μM)	**7.1 ± 0.2**	**29.9 ± 5.7$^{\#}$**	**7**
4. Vehicle + L-NAME / ODQ, indomethacin + Pyr3	**-**	**26.0 ± 12.1$^{\#}$**	**5**

Figure S6. Endothelium-dependent relaxation in rat mesenteric artery. In pressurized rat mesenteric arteries, relaxation to ACh (1 nM-100 μM) was examined in the absence (*A*) and presence (*B*) of Pyr3 (1 μM) in the absence (*A, B,* circles) and presence (*A, B,* triangles) of L-NAME (100 μM), ODQ (10 μM) and indomethacin (10 μM) to clarify the relative potential contribution of TRPC3 to EDH, and NO/prostaglandin-mediated relaxation. Each *n* is from a different animal. $P<0.05$ indicates difference in *, for 0.3 μM ACh (in *B*); **pEC_{50}, between controls (in *A*; see also *C*); $^{\#}E_{max}$, relative to matched ACh controls (*C*). Data for + L-NAME, ODQ and indomethacin are from *Figure 2* and *Table 3*.

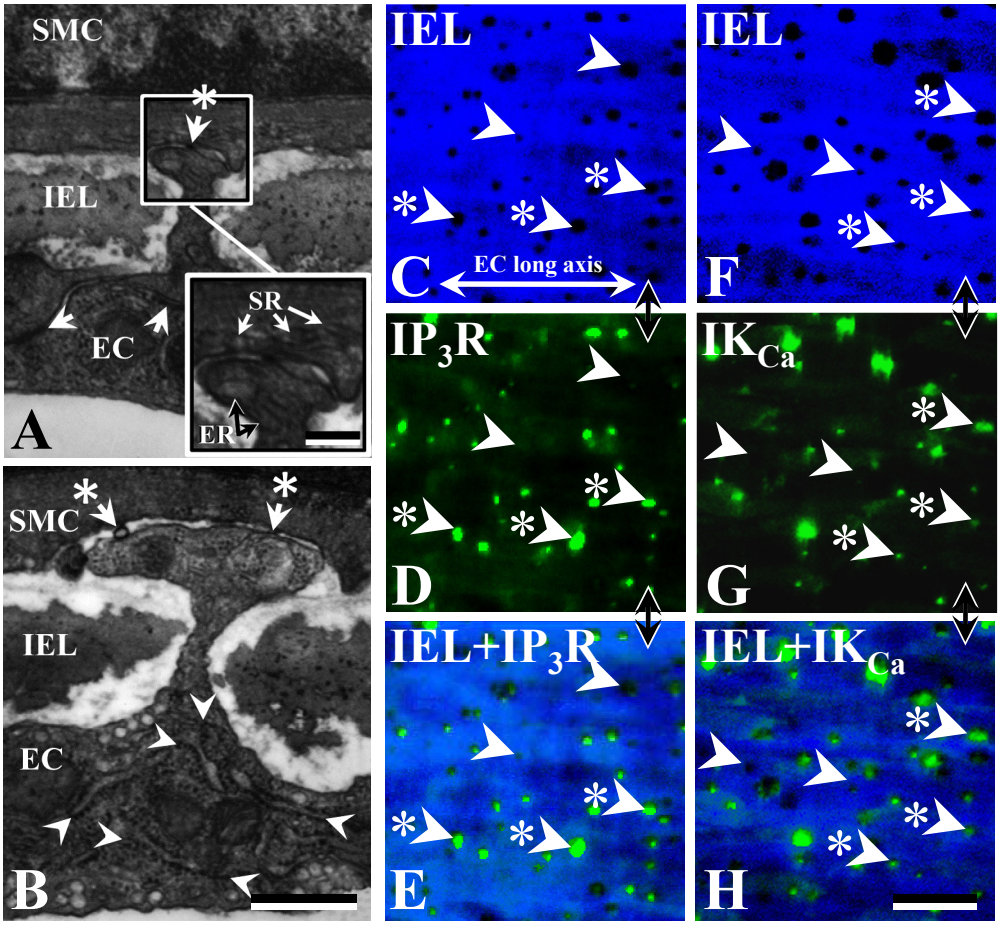

Figure S7. Ultrastructure of selected close myoendothelial contact sites and confocal immunohistochemistry of IP_3R and IK_{Ca} in rat mesenteric artery. At selected endothelial cell (EC) and smooth muscle cell (SMC) contact sites of ≤30 nm, smooth endoplasmic and sarcoplasmic reticulum (ER/SR; *A*) and rough ER (*B*; arrowed) are present in and near the associated EC projection (*A, B*). Small regions of myoendothelial gap junction membrane are also present (arrow with asterisk, A and inset; *B*), as are EC-EC gap junctions near such sites. Of note, in rat mesenteric artery, only a proportion of close myoendothelial contact sites have apparent accumulations of ER and / or SR. In a similar manner, inositol-1,4,5-trisphosphate receptor (IP_3R) and intermediate conductance calcium-activated potassium channel (IK_{Ca}, as IK1) are localized to a proportion of internal elastic lamina (IEL) hole sites (dark spots), at the IEL-SM focal plane border, as potential sites of close myoendothelial contact (*C-E* and *F-H*, respectively; examples at arrowheads with asterisks; using antibodies to pan-IP_3R and IK1, from Chemicon (AB1622) and Craig Neylon,[21] University of Melbourne (respectively). Lower level diffuse IP_3R and IK_{Ca} is also localized to the endothelial membrane (*D, G,* respectively). IEL holes without accumulations of IP_3R or IK_{Ca} are also present (*C-H,* examples at arrowheads without asterisks). Of note, IEL panels (*C, F*) have been contrast/brightness enhanced in Photoshop. Peptide block and incubation in secondary antibody alone resulted in no labelling (data not shown), with antibody characterization, as per previous studies.[4,6,22] Longitudinal vessel axis left to right, with *n*=3, each from a different animal (*C-H*). Scale bars, 1 μm (*A, B* main), inset, 200 nm (*B*), 25 μm (*C-H*). Data from adult male rat second and third order vessels. Panels *A-E* from,[23] with permission; *F-H,* Sandow, unpublished results (see also[4,6,24]).